ISSN 0016-7029, Geochemistry International, 2011, Vol. 49, No. 11, pp. 1085–1110. © Pleiades Publishing, Ltd., 2011.
Original Russian Text © M.V. Portnyagin, V.B. Naumov, N.L. Mironov, I.A. Belousov, N.N. Kononkova, 2011, published in Geokhimiya, 2011, Vol. 49, No. 11, pp. 1153–1178.

Composition and Evolution of the Melts Erupted in 1996 at Karymskoe Lake, Eastern Kamchatka: Evidence from Inclusions in Minerals

M. V. Portnyagin[a, b], V. B. Naumov[a], N. L. Mironov[a], I. A. Belousov[a], and N. N. Kononkova [a]

[a] *Vernadsky Institute of Geochemistry and Analytical Chemistry, Russian Academy of Sciences, ul. Kosygina 19, Moscow, 119991 Russia*

e-mail: mportnyagin@geokhi.ru, naumov@geokhi.ru

[b] *Leibnitz Institute of Marine Research, IFM-GEOMAR, Wischhofstr. 1–3, D-24148 Kiel, Germany*

e-mail: mportnyagin@ifm-geomar.de

Received March 5, 2010

Abstract—The powerful eruption in the Akademii Nauk caldera on January 2, 1996, marked a new activity phase of Karymsky volcano and became a noticeable event in the history of modern volcanism in Kamchatka. The paper reports data obtained by studying more than 200 glassy melt inclusions in phenocrysts of olivine ($Fo_{82–72}$), plagioclase ($An_{92–73}$), and clinopyroxene (Mg# 83–70) in basalts of the 1996 eruption. The data were utilized to estimate the composition of the parental melt and the physicochemical parameters of the magma evolution. According to our data, the parental melt corresponded to low magnesian, highly aluminous basalt ($SiO_2 = 50.2$ wt %, MgO = 5.6 wt %, $Al_2O_3 = 17$ wt %) of the mildly potassic type ($K_2O = 0.56$ wt %) and contained much dissolved volatile components ($H_2O = 2.8$ wt %, S = 0.17 wt %, and Cl = 0.11 wt %). Melt inclusions in the minerals are similar in chemical composition, a fact testifying that the minerals crystallized simultaneously with one another. Their crystallization started at a pressure of approximately 1.5 kbar, proceeded within a narrow temperature range of 1040 ± 20°C, and continued until a near-surface pressure of approximately 100 bar was reached. The degree of crystallization of the parental melt during its eruption was close to 55%. Massive crystallization was triggered by H_2O degassing under a pressure of less than 1 kbar. Magma degassing in an open system resulted in the escape of 82% H_2O, 93% S, and 24% Cl (of their initial contents in the parental melt) to the fluid phase. The release of volatile compounds to the atmosphere during the eruption that lasted for 18 h was estimated at 1.7×10^6 t H_2O, 1.4×10^5 t S, and 1.5×10^4 t Cl. The concentrations of most incompatible trace elements in the melt inclusions are close to those in the rocks and to the expected fractional differentiation trend. Melt inclusions in the plagioclase were found to be selectively enriched in Li. The Li-enriched plagioclase with melt inclusions thought to originate from cumulate layers in the feeding system beneath Karymsky volcano, in which plagioclase interacted with Li-rich melts/brines and was subsequently entrapped and entrained by the magma during the 1996 eruption.

Keywords: Karymsky volcano, Kamchatka, melt inclusions.

DOI: 10.1134/S0016702911110085

INTRODUCTION

Karymsky volcano, which belongs to the Karymsky volcanic center, is one of the most currently active volcanoes in Kamchatka. It is characterized by contrasting basaltic and andesitic volcanism, as during the 1996 eruption, which initially proceeded at two interrelated centers (Karymskoe Lake and Karymsky volcano). The petrology of the products erupted at modern time in the Karymsky center was extensively discussed in several recent publications [1–6]. Based on the geochemistry of the rocks and the composition of their minerals and melt inclusions in them, it has been demonstrated that the basalts and andesites of the Karymsky center are closely interrelated by the fractional crystallization of a single basaltic magma, whose injection into a crustal andesitic chamber likely triggered the eruption of Karymsky stratovolcano, which continues until nowadays [3–5].

Data on the composition of melt inclusions in plagioclase from andesites and basalts from the Karymsky center generally corroborate the conclusion that the rocks are genetically interrelated [2, 6] but also made it possible to reveal certain features that have never been indetified in melt inclusions in minerals from other volcanoes in Kamchatka. It was the most unusual and hard to explain that the primitive melt inclusions of basalt composition in plagioclase from Karymsky volcano are significantly enriched in Na (>6 wt %) and Li (>100 ppm) relative to the rocks and more differentiated melts. In spite of their primitive basaltic composition, such melts could not be parental for the rocks of Karymsky volcano. The petrogenetic meaning of these facts and the actual composition of the parental melt, as

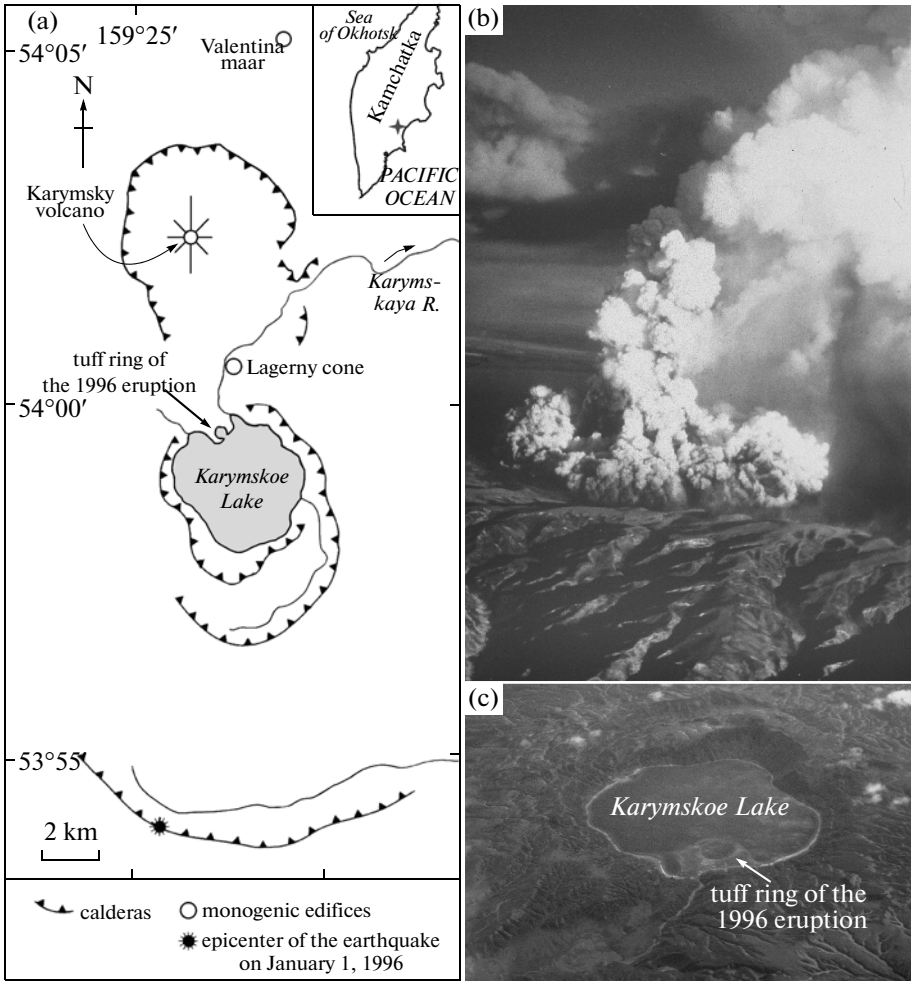

Fig. 1. Geological setting of the 1996 eruption in the Akademii Nauk caldera. Schematic geological map of the Karymsky volcanic center. The inset shows the location of Karymsky volcano in Kamchatka.
Eruption on January 2, 1996 (photo: Ya.D. Murav'ev). Karymskoe Lake as can be seen nowadays (photo: A.B. Belousov).
Figures 1a and 1c show the tuff ring produced by the 1996 eruption at Karymskoe Lake.

well as the conditions of its evolution before the eruption, remain uncertain up to now. Also, it is unclear as to which roles were played by crustal assimilation and the melting of basement rocks in the origin of the contrasting basalt–andesite association of the Karymsky volcanic center [1, 7].

This publication presents our detailed data on the composition of naturally quenched melt inclusions in rock-forming minerals (olivine, plagioclase, and clinopyroxene) in basalts of the 1996 eruption of Karymsky volcano, including the contents of volatiles and trace elements. These data allowed us to estimate the physicochemical parameters of melt evolution prior to and during the eruption and to evaluate the extent of melt degassing and the emission of volatile components. We have also developed a model for Li selective enrichment in melt inclusions in the plagioclase.

VOLCANIC CENTER AND ITS ROCKS

The Karymsky volcanic center in the frontal part of the central segment of the Eastern Volcanic Belt in Kamchatka is located approximately 120 km northeast of the city of Petropavlovsk-Kamchatskii (Fig. 1a). The distance between the volcanic center and the Pacific plate subducted beneath Kamchatka is close to 125 km, i.e., 15–25 km greater than those for other active frontal volcanoes in Kamchatka [8].

The Karymsky center comprises numerous Pliocene–Quaternary volcanic edifices of differentiated composition [9] and a series of ring structures, which are eccentrically "interleaved" and were formed during catastrophic eruptions of pumice–ignimbrite acid pyroclastic material [1]. Modern volcanic activity in the territory is focused mostly at the Karymsky andesite stratovolcano, which sits in the Karymsky caldera dated at 7900 ^{14}C years B.P. [10]. Karymskoe Lake 6 km south of the volcano fills the Late Pleistocene

Table 1. Representative analyses (wt %) of olivine in basalt of the 1996 eruption

Component	Sample KR96BV				Sample KR99/96				
	1	2	3	4	5	6	7	8	9
SiO_2	39.19	37.97	37.78	37.69	38.89	38.95	38.82	37.79	37.81
FeO	17.90	21.88	23.48	25.67	17.43	17.91	18.08	22.54	22.98
MnO	0.27	0.35	0.38	0.44	0.19	0.26	0.34	0.36	0.42
MgO	43.50	40.29	38.64	36.70	43.49	42.47	42.44	38.98	38.86
CaO	0.18	0.18	0.18	0.18	0.16	0.18	0.21	0.18	0.15
Cr_2O_3	0.03	0.01	0.02	0.01	0.00	0.05	0.04	0.03	0.01
NiO	0.08	0.08	0.02	0.07	0.07	0.06	0.09	0.07	0.08
Total	101.15	100.76	100.50	100.76	100.23	99.88	100.02	99.95	100.31
Fo	81	77	75	72	82	81	81	76	75

Akademii Nauk caldera, which is situated in the caldera of Odnobokova volcano, dated at approximately 70 ka [11] (Fig. 1a).

The latest (and continuing nowadays) eruption of Karymsky volcano began on January 2, 1996. The subsequent (a few hours later) eruption in the northern part of Karymskoe Lake lasted for about 18 h, and the 0.04 km^3 of the ejected volcanic material has a predominantly basalt composition. The eruption was of explosive phreatomagmatic character (Fig. 1b), and its products are volcanic sand, lapilli, and bombs up to 70 cm across [12, 13]. The eruption produced a tuff ring about 1 km in diameter (Fig. 1c).

The basalts of the 1996 eruption are black porous (20–30%) glassy rocks abounding (30–35%) in plagioclase phenocrysts (Fig. 2a). Olivine and clinopyroxene are contained in the rocks in varying amounts and account for 5–10% of the rocks by volume. The phenocrysts comprise two populations: phenocrysts 0.6–2.5 mm and subphenocrysts 0.2–0.4 mm. The plagioclase phenocrysts are broad tablets with slightly rounded contours and usually contain melt inclusions. The olivine and clinopyroxene phenocrysts are often fractured and contain rare melt and crystalline inclusions and groundmass embayments. The groundmass of the rocks has a hyalitic (pialotaxitic) texture and consists of dark brown glass (60%) with submerged elongated microlites of plagioclase (32%), clinopyroxene (7%), and magnetite (1%).

We examined melt inclusions in minerals in two basaltic tephra samples from the 1996 eruption, which were made available for us by courtesy of A.B. Belousov. The samples represent small (1–2 cm) lapilli from the deposits of the basic wave (sample KR96BV) and a volcanic bomb (sample KR99/96).

METHODS

Melt inclusions were studied in olivine, plagioclase, and pyroxene phenocrysts. Representative analyses of these minerals are reported in Tables 1–3. The olivine phenocrysts usually contain single inclusions or their groups (comprising five to ten inclusions), with the inclusions reaching 150 μm across. Inclusions in olivine are rounded and ellipsoidal (Figs. 2b–2e), sometimes showing faceting of negative olivine crystals or, more rarely, having irregular shapes (Fig. 2c) and consist of pale or dark brown glass. Inclusions in relatively magnesian olivine (Fo_{81-80}) contain fluid bubbles, which account for up to 2.5% of the inclusions by volume (Figs. 2b–2d). The size of the bubbles decreases in more ferrous olivine (Fo_{77}) to approximately 1% (Fig. 2d). Inclusions in the most ferrous olivine (Fo_{74-75}) are completely homogeneous (Fig. 2e). Some inclusions contain crystalline phases (magnetite and plagioclase) (Fig. 2c).

Inclusions occur in the pyroxene as groups of up to a few dozen inclusions, which are chaotically distributed within the crystals or, more rarely, are prone to be spatially restricted to growth zones (Figs. 2g–2i). The inclusions are rounded, slightly elongated, or irregular in shape and usually contain single small contraction bubbles or are completely homogeneous.

Inclusions in the plagioclase are usually very abundant, broadly vary in size, are evenly distributed over the volume of the host crystals, and occur in association with low-density fluid inclusions (Fig. 2f). The inclusions are flattened, irregular (along other directions), rounded, or elongated (along growth zones of the crystals) and consist of pale brown glass. Large (>50 μm) melt inclusions usually contain two or three small gas bubbles, and smaller inclusions contain only one bubble. No correlations were detected between the variations in the morphology of the inclusions and the composition of the host mineral.

In order to study melt inclusions, we hand-picked olivine, pyroxene, and plagioclase crystals from the crushed nonmagnetic size fraction 0.5–1 mm. Mineral grains were then mounted in epoxy pellets, which were polished with corundum powders and diamond pastes.

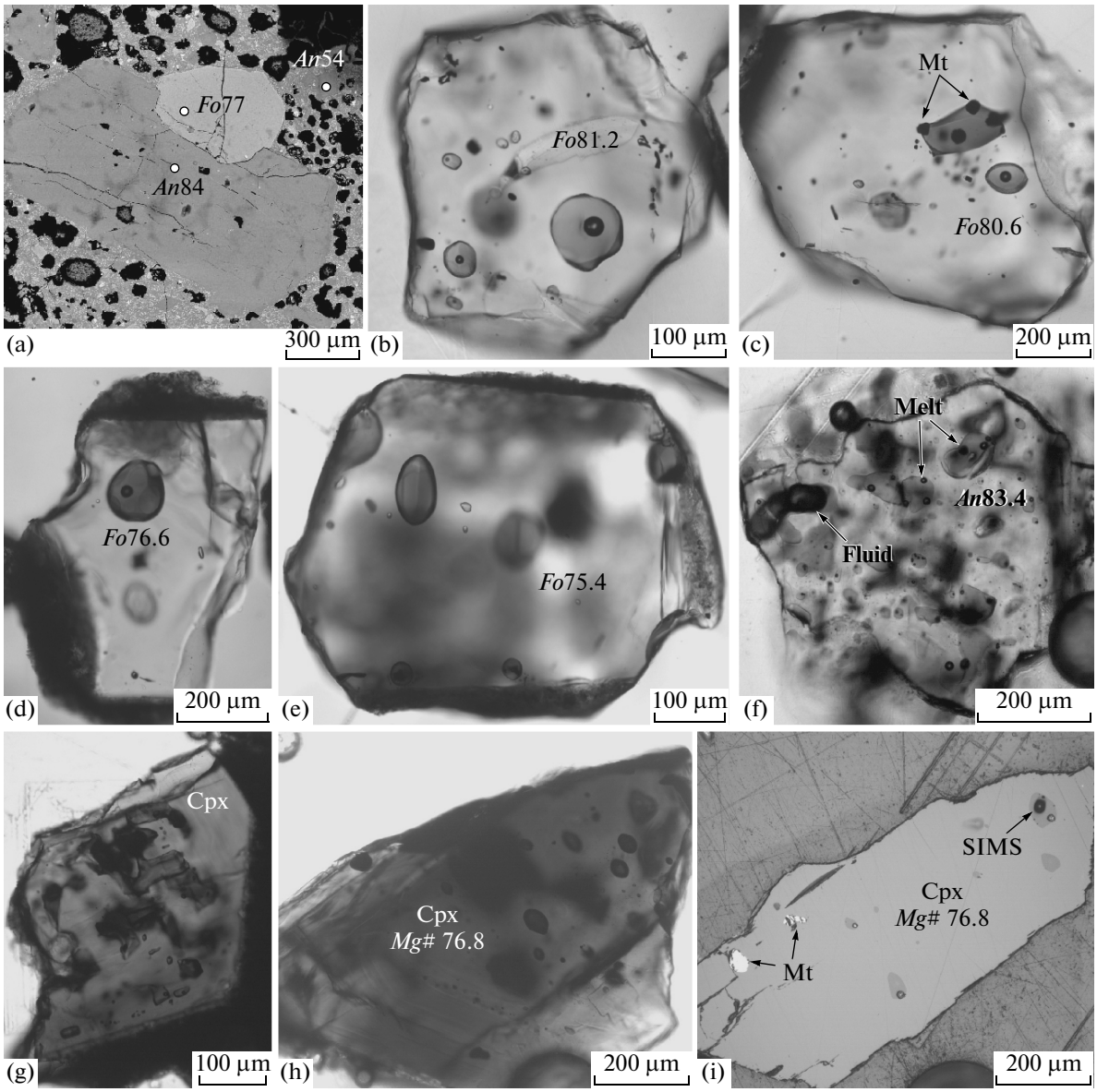

Fig. 2. Micrographs and BSE images of our samples. BSE image of an aggregate of plagioclase and olivine crystals in basalt of the 1996 eruption. Circles mark analytical spots. (b–e) Melt inclusions in olivine. (f) Melt inclusion in plagioclase. (g–i) Melt inclusions in clinopyroxene. Figures 2b–2h are micrographs in transmitted light, Fig. 2i is transmitted-light micrograph. Arrows in Fig. 2i point to the ion-probe analytical crater.

Inclusions exposed at the surface were analyzed for major elements on an electron microprobe and for trace elements on an ion probe.

Concentrations of major elements, S, and Cl in melt inclusions and the compositions of minerals were analyzed on a Cameca SX-100 microprobe at the Vernadsky Institute of Geochemistry and Analytical Chemistry, Russian Academy of Sciences. Glasses were analyzed using a defocused beam, by scanning over an area of 5×5 or 12×12 μm at 30 nA current and 15 kV accelerating voltage. Spot analyses of minerals were carried out at a current of 30 nA and accelerating voltage of 15 kV. To unify and control the quality of the analyses, we used standard reference samples of natural minerals and glasses [14]. Within the scope of this research, we have analyzed 97 inclusions in olivine, 86 in plagioclase, and 25 in clinopyroxene. Minerals were analyzed in polished petrographic thin sections at the Laboratory of Local Analytical Techniques at the Department of Petrology of the Moscow State University on a CamScan 4DV scanning electron microscope equipped with a LinkSystem 10 000 EDS analytical setup.

Concentrations of trace elements (Li, B, Be, Cr, V, Ti, Zr, Y, Nb, Ba, La, Ce, Nd, Sm, Eu, Gd, Dy, Er, Yb, Hf, Th, U, and Pb), H_2O, and F in the glass of melt inclusions (19 inclusions in olivine, seven in plagioclase, and seven in pyroxene) and in the matrix glass

Table 2. Representative analyses (wt %) of clinopyroxene in basalt of the 1996 eruption

Component	Sample KR96BV					Sample KR99/96				
	1	2	3	4	5	6	7	8	9	10
SiO_2	51.68	51.15	52.06	51.16	50.61	51.66	51.26	51.88	51.79	51.11
TiO_2	0.48	0.61	0.47	0.47	0.55	0.50	0.53	0.45	0.53	0.53
Al_2O_3	2.53	3.00	2.12	3.38	3.22	2.63	2.93	2.16	1.96	3.22
Cr_2O_3	0.02	0.03	0.02	0.28	0.06	0.03	0.18	0.03	0.00	0.00
FeO	8.75	8.77	8.84	6.94	7.99	8.51	7.77	9.08	9.77	7.92
MnO	0.28	0.27	0.31	0.20	0.21	0.25	0.21	0.32	0.38	0.20
MgO	16.29	15.45	15.99	15.67	14.98	15.84	15.77	16.21	15.05	15.19
CaO	19.85	20.53	20.14	21.64	21.51	20.43	20.94	19.48	20.19	21.63
Na_2O	0.23	0.26	0.28	0.26	0.23	0.26	0.29	0.27	0.32	0.29
Total	100.11	100.08	100.23	100.00	99.36	100.11	99.87	99.89	99.98	100.09
Mg#	77	77	76	80	77	77	78	76	73	77

Table 3. Representative analyses (wt %) of plagioclase in basalt of the 1996 eruption

Component	Sample KR96BV					Sample KR99/96				
	1	2	3	4	5	6	7	8	9	10
SiO_2	43.50	44.24	45.74	46.39	48.19	42.90	43.91	45.33	46.11	45.99
Al_2O_3	35.64	35.17	34.27	33.58	32.36	35.59	35.03	34.55	34.00	33.18
FeO	0.58	0.68	0.73	0.74	0.68	0.62	0.65	0.67	0.72	0.71
CaO	18.56	18.49	17.38	16.45	15.37	19.21	18.60	17.66	17.16	16.60
Na_2O	1.14	1.31	1.94	2.40	3.03	0.91	1.33	1.68	2.06	2.45
K_2O	0.00	0.05	0.05	0.06	0.12	0.01	0.01	0.04	0.04	0.06
Total	99.42	99.94	100.11	99.62	99.75	99.24	99.53	99.93	100.09	98.99
An	90	88	83	79	73	92	89	85	82	79

were analyzed by secondary ion mass spectrometry on a Cameca ims4f ion probe at the Yaroslavl Branch of the Physical–Technological Institute, Russian Academy of Sciences. Specifics and technicalities of the analytical procedure are described in much detail in [15, 16]. The quality of the analyze was monitored using NIST610 [17] and KL2G [18] standard reference samples in the same series as the samples to be analyzed.

The composition of melt inclusions in olivine was corrected for their equilibria with the host mineral by means of "backward modeling" the fractional crystallization of olivine until the melt reached equilibrium with the composition of the host mineral. The simulations were carried out with the Petrolog 2.13 program package [19]. The amount of olivine added to the melt to reach equilibrium did not exceed 8 mol %and was less than 3 mol % for 68 inclusions of the whole set of 92. The composition of melt inclusions in plagioclase was not corrected. As was discussed above, the absence of systematic differences in the compositions of melt inclusions in various minerals testifies that the compositions of these inclusions have not been any significantly modified by olivine crystallization on the walls of the inclusions.

RESULTS

Major elements. The compositions of minerals in which melt inclusions were analyzed spread over broad enough ranges: $Fo_{82–72}$ for olivine, $An_{92–73}$ for plagioclase, and Mg# 83–70 for pyroxene (Fig. 3). Inclusions in these three minerals mostly have a basaltic or basaltic andesitic composition (Tables 4–7, Fig. 4). The compositions of both the rocks and the inclusions correspond to the mildly potassic island-arc series [20]. The most primitive basaltic compositions were analyzed in the olivine, and conversely, the most evolved (up to andesitic) compositions were identified in inclusions in the plagioclase and pyroxene. Inclusions of intermediate composition are similar in all of these minerals. Similar values were also obtained for the average compositions of melt inclusions in various phases (Table 8).

The SiO_2 concentration of the melt inclusions increases with decreasing *Mg#* of the olivine and pyrox-

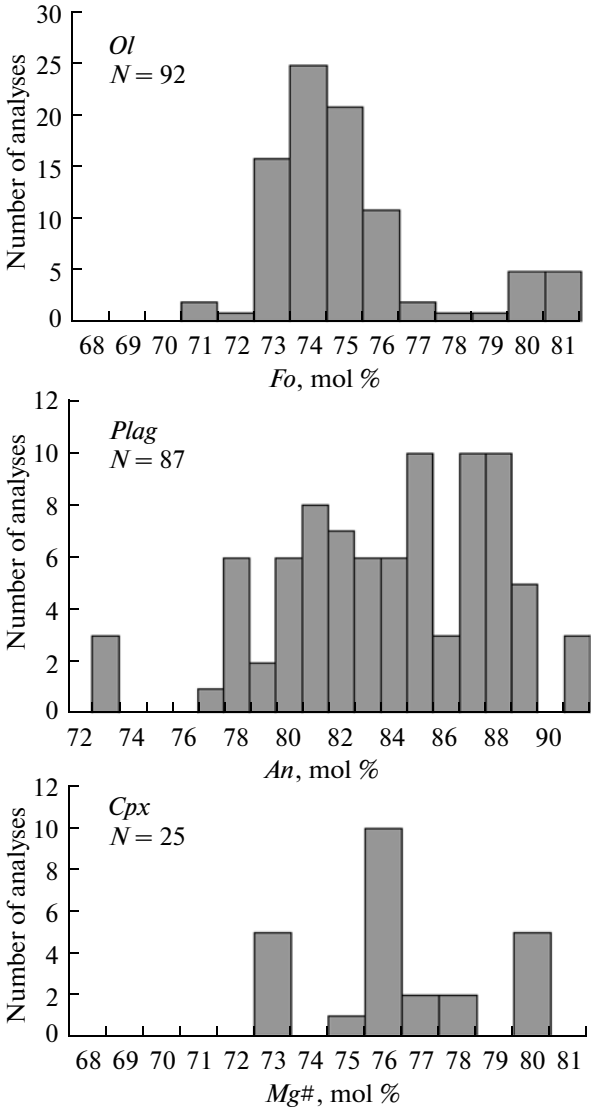

Fig. 3. Histograms showing the distribution of the compositions of minerals hosting melt inclusions. *N* is the number of analyses of melt inclusions in each mineral.

ene and decreasing anorthite concentration of the plagioclase and is obviously correlated with the MgO, CaO (negative correlation), and K_2O (positive correlation) concentrations. Other elements exhibit a somewhat broader scatter of their concentrations, but the Na_2O and TiO_2 concentrations are generally prone to increase with increasing SiO_2 concentration, while the FeO and Al_2O_3 concentrations, conversely, decrease (Fig. 4). The Al_2O_3 concentrations of the inclusions vary within a much broader range, which is likely explained by the effect of crystallization or melting processes of the host minerals after the capture of the inclusions. The groundmass glasses of the rocks have an andesitic composition (SiO_2 = 56.7–59.6 wt %) close to those of the most evolved inclusions in the plagioclase and pyroxene and plot on the continuations of the trends of the melt inclusions (Fig. 4).

In terms of concentrations of most major elements, the inclusions have a comparable or slightly more differentiated composition than the basalts of the 1996 eruption but a less differentiated composition than that of the andesites of Karymsky volcano (Fig. 4). The TiO_2 and FeO concentrations of the inclusions are systematically higher than in the rocks. The Al_2O_3 concentrations are prone to deviate below the line connecting the andesite and basalt compositions. Compared to the compositions of inclusions in plagioclase in basalts of the 1996 eruption [2], the inclusions exhibit narrower compositional ranges. We found no Na- and K-rich and Fe-poor compositions, which were reported in [2], a fact testifying to differences between the compositions of inclusions in the plagioclase from various basalt samples of the 1996 eruption.

Volatile components. The H_2O contents of the inclusions (Tables 9–11) vary from 1.6 to 3.9 wt % and are not correlated with the concentrations of any major components or the composition of the host mineral (Fig. 5a). The broadest compositional range and the highest concentrations were detected in inclusions in olivine. The H_2O concentrations of inclusions in plagioclase and pyroxene vary within narrower ranges (1.7–2.9 wt %). Our estimates of the H_2O contents generally lie within the usual ranges of values of primitive melts in Kamchatka [16]. The maximum H_2O/K_2O ratios of about 5 (±20%) of inclusions was assumed as characteristic of the parental minimally degassed melt. The H_2O concentration of the groundmass glass are systematically lower than in the inclusions and are ~1.1 wt %.

The sulfur concentrations of most inclusions are 0.20–0.03 wt % and rapidly decrease with increasing K_2O and SiO_2 concentrations (Fig. 5b). The maximum S concentrations of 0.3 wt % were found in rare inclusions in plagioclase. Some inclusions in plagioclase shown in Fig. 5b deviate from the nearly vertical trend toward somewhat elevated K_2O concentrations and toward the composition of inclusions in plagioclase from andesites of Karymsky volcano. The maximum S/K_2O ratio of ~0.35 is similar in inclusions in all of the three minerals. The S concentration of the groundmass glass and the most strongly evolved melt inclusions is 0.02–0.04 wt %, i.e., is slightly lower than in differentiated andesite inclusions in plagioclase from andesites of Karymsky volcano (0.04–0.15 wt %) [2].

The concentrations of Cl in inclusions in olivine lie within a narrow range of 0.08–0.15 wt % and very insignificantly increase with increasing K_2O concentration (Fig. 5c). The composition of the groundmass glass (~0.14 wt % Cl) plots on the continuation of the trend of the melt inclusions. The composition of inclusions in pyroxene and plagioclase shows a higher dispersion, but the average values are close to those of inclusions in oli-

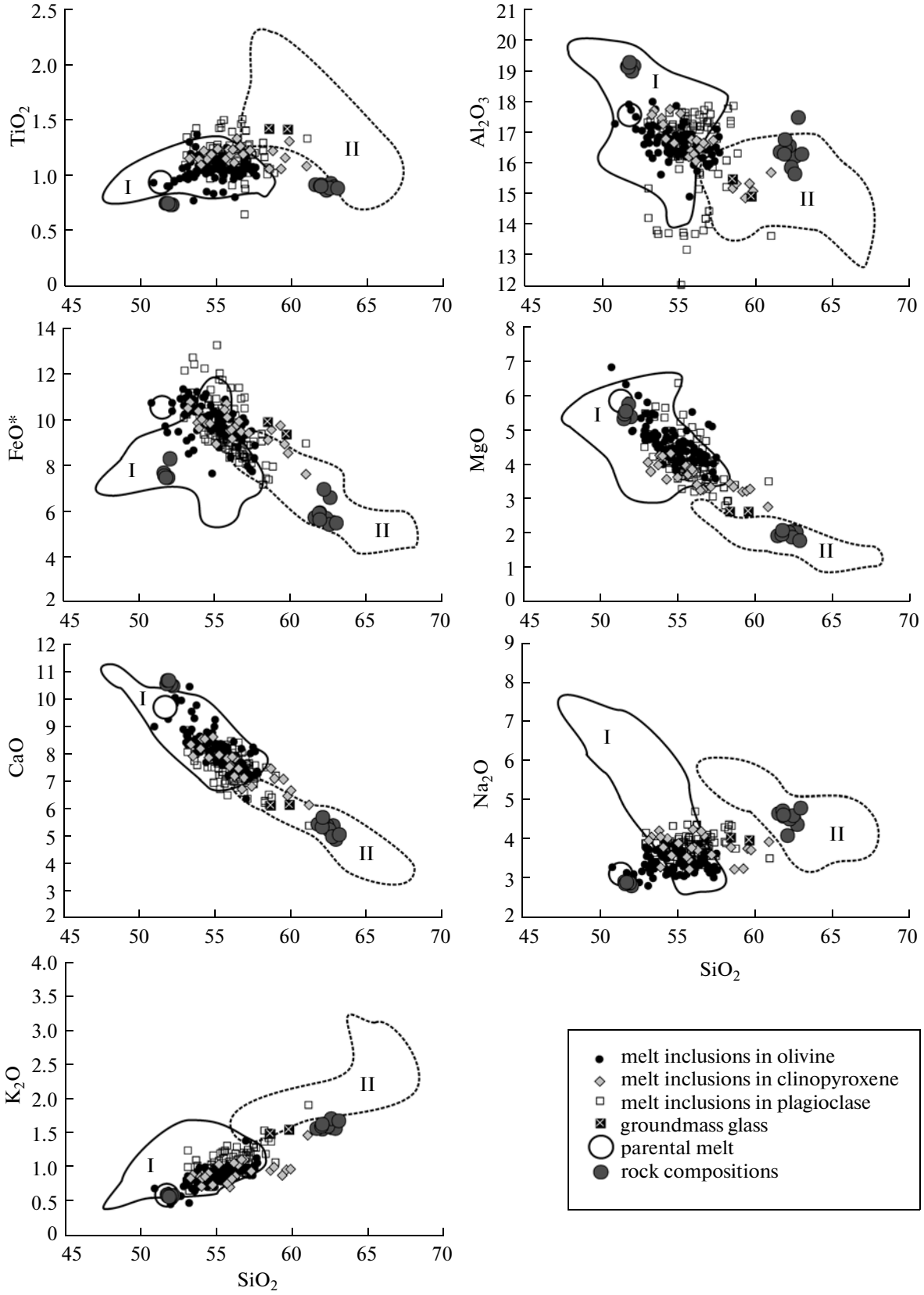

Fig. 4. Concentrations of major components in melt inclusions. Fields show the composition of melt inclusions in plagioclase from (I) basalt of the 1996 eruption and (II) andesite of the 1996 eruption of Karymsky volcano according to [2]. The compositions of basalt of the 1996 eruption and andesite erupted by Karymsky volcano during the time span from 1963 through 1999 are given according to [4].

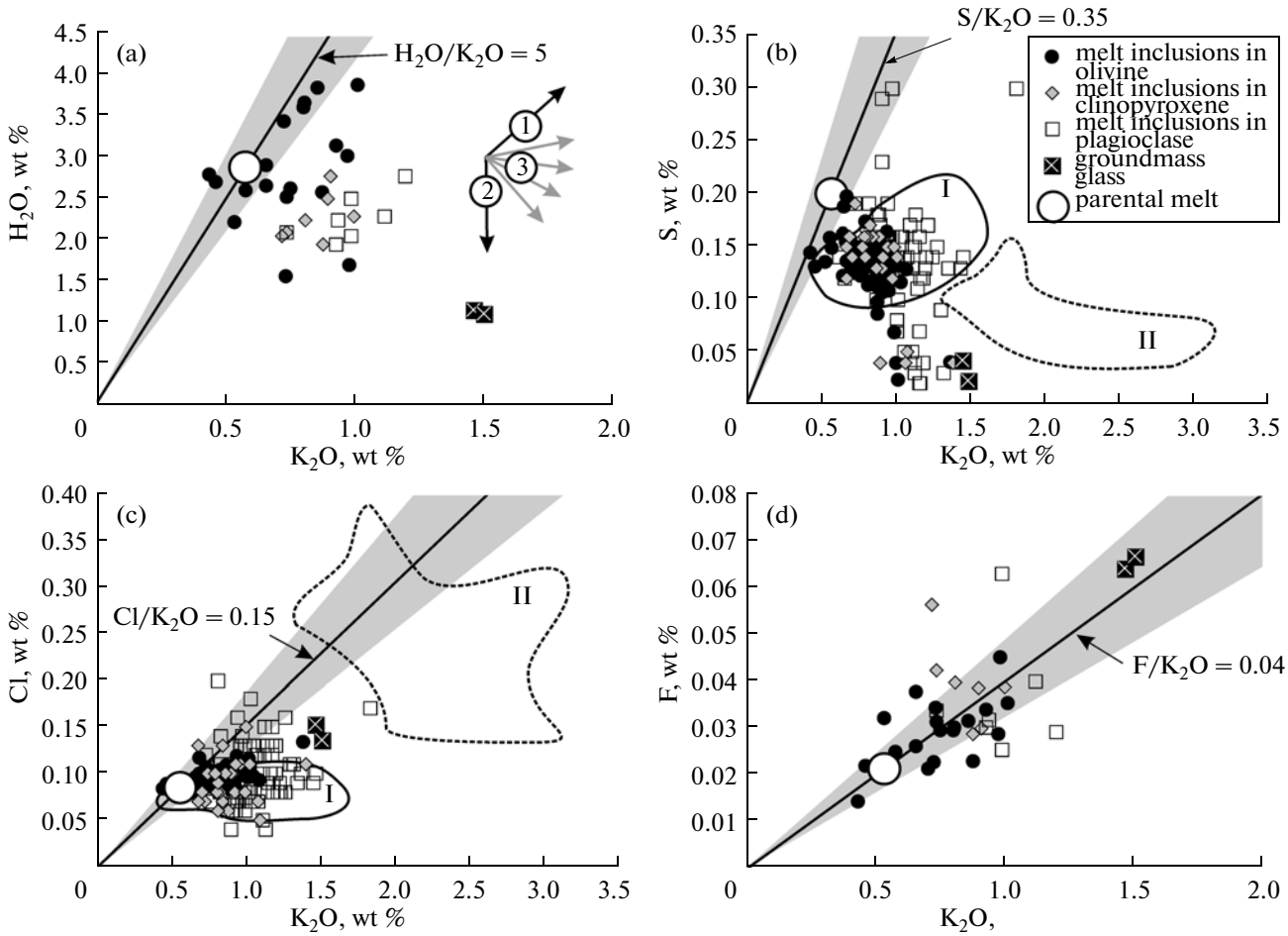

Fig. 5. Systematics of volatile components in melt inclusions.

Fields in Figs. 5a and 5b show the compositions of melt inclusions in plagioclase from (I) basalts of the 1996 eruption and (II) andesite of Karymsky volcano, according to [2]. Heavy lines show the maximum volatile/K_2O ratios assumed to evaluate the parental melt composition. The shaded field shows the probable error range of the estimates (±20). Arrows in Fig. 5a show various evolution scenarios for the concentrations of volatile components in the magmatic systems: (*1*) closed crystallization system, with the residual melt enriched in volatile components; (*2*) melt degassing without crystallization; (*3*) various crystallization scenarios coupled with melt degassing.

vine. All inclusions in minerals from rocks of the 1996 eruption (this publication and [2]) have Cl concentrations systematically lower than those in inclusions in plagioclase from andesites of Karymsky volcano (0.14–0.38 wt %), but the range of the Cl/K_2O ratio (0.05–0.20) is practically the same in all inclusions in basalts and andesites of the Karymsky center.

In contrast to the concentrations of other volatile compositions, the F concentrations in the inclusions (0.015–0.063 wt %) correlat with K_2O (Fig. 5d). The F/K_2O ratio of 0.04 remains practically unvarying throughout the whole compositional range of the inclusions and corresponds to the composition of the matrix glass.

Trace elements. The concentrations of incompatible trace elements in the melt inclusions are close to the compositions of basalts of the 1996 eruption and show a distribution typical of basalt–andesite melts in Kamchatka and arc magmas as a whole ([16], Fig. 6). The concentrations of incompatible trace elements of the matrix glass are roughly 2–2.5 times higher than in the rocks. The compositions of most of the melt inclusions are intermediate between the compositions of the rocks and matrix glass. The only exception is Sr, whose concentrations in the matrix glass is 1.5 times lower than in the rock and decreases in the inclusions with increasing K_2O and SiO_2 concentrations. All inclusions differ from the basalts in having no pronounced Ti minimum with respect to REE in the normalized patterns and in having slightly lower Sr/Ce ratios: the Sr_N/Ce_N ratios of the inclusions are 0.9–2.4, while those of the basalts are 3.1 (the subscript index N denotes concentrations normalized to those in the mantle).

The compositions of melt inclusions in the olivine, pyroxene, and plagioclase (Figs. 6a–6c) are similar (within the analytical error of approximately 20%) in terms of concentrations of most incompatible elements.

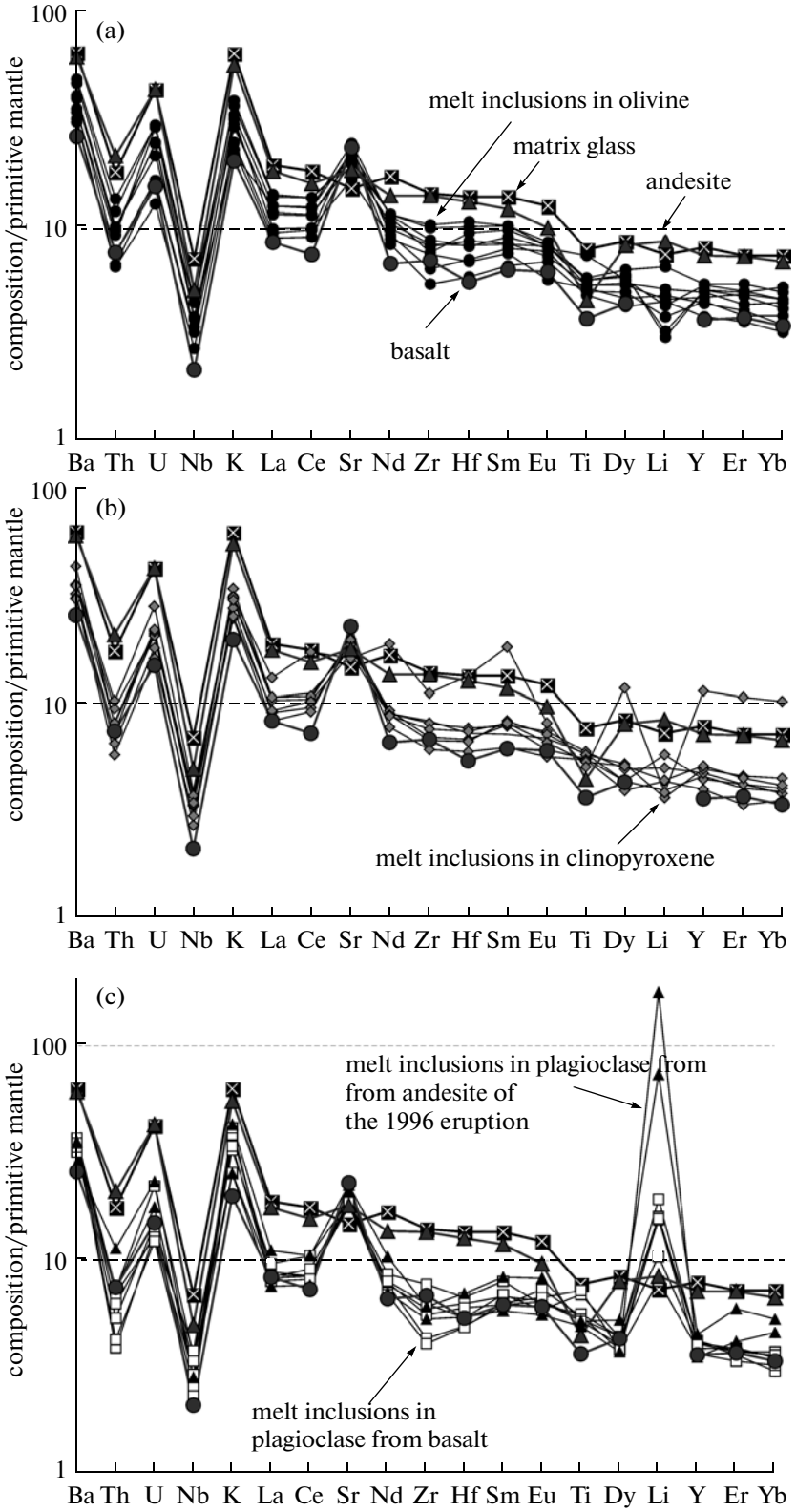

Fig. 6. Primitive mantle-normalized [23] trace-element patterns of melt inclusions. Melt inclusions in olivine; (b) melt inclusions in pyroxene; (c) melt inclusions in plagioclase. All plots show, for comparison, the average composition of basalts of the 1996 eruption and andesites erupted in 1963–1996 by Karymsky volcano [4] and the composition of the matrix glass. Figure 6c additionally exhibits the compositions of melt inclusions in plagioclase from andesites of the 1996 eruption [2, 3].

Table 4. Chemical composition (wt %) of glass in melt inclusions in olivine from basalt (sample KR96BV) from the Karymsky volcanic center

Inclusion no.	Component												Total	*Fo*
	SiO_2	TiO_2	Al_2O_3	FeO	MnO	MgO	CaO	Na_2O	K_2O	P_2O_5	Cl	S		
1	49.00	1.09	19.02	10.00	0.16	3.81	9.63	3.51	0.73	0.14	0.10	0.14	97.24	82
2	49.03	0.88	17.81	9.10	0.11	4.89	10.23	2.84	0.44	0.14	0.08	0.14	95.70	81
3	50.75	1.01	17.38	9.88	0.18	3.65	8.81	3.73	0.79	0.18	0.10	0.14	96.60	76
4	50.77	0.97	18.63	9.14	0.16	2.55	10.41	3.09	0.57	0.14	0.10	0.16	96.68	76
5	50.83	1.32	16.74	10.17	0.19	4.38	8.06	3.26	0.74	0.21	0.09	0.14	96.12	76
6	50.92	0.98	17.38	9.91	0.09	3.83	8.73	3.27	0.81	0.11	0.08	0.17	96.29	76
7	51.05	1.27	17.07	10.45	0.20	4.36	8.21	3.16	0.80	0.17	0.09	0.15	96.97	76
8	51.16	0.97	17.31	9.86	0.23	3.90	8.51	3.70	0.84	0.14	0.09	0.15	96.84	76
9	51.21	1.24	17.02	8.33	0.16	4.37	9.67	3.35	0.68	0.14	0.12	0.20	96.48	81
10	51.29	0.96	16.80	10.61	0.24	4.14	8.39	3.17	0.68	0.17	0.10	0.14	96.69	75
11	51.46	0.98	17.34	10.12	0.17	3.62	8.74	3.81	0.82	0.14	0.10	0.13	97.43	77
12	51.48	1.07	17.54	9.31	0.23	3.84	8.51	3.66	0.82	0.16	0.09	0.14	96.85	76
13	51.54	1.03	17.67	9.62	0.19	3.51	9.06	3.67	0.82	0.10	0.10	0.14	97.46	79
14	51.65	1.02	17.41	9.35	0.19	3.86	8.35	3.50	0.78	0.19	0.10	0.14	96.53	76
15	51.68	1.02	17.26	9.43	0.18	3.64	8.24	3.44	0.81	0.23	0.09	0.15	96.18	75
16	51.73	1.11	17.28	10.28	0.21	3.48	8.57	3.87	0.87	0.18	0.11	0.15	97.99	77
17	51.75	0.98	17.12	10.33	0.21	4.17	8.01	3.29	0.73	0.22	0.10	0.13	97.03	75
18	51.90	1.01	16.96	8.85	0.21	4.29	8.03	3.24	0.80	0.21	0.09	0.14	95.73	77
19	52.00	1.02	17.02	8.57	0.17	4.30	7.70	3.41	0.84	0.20	0.09	0.14	95.46	77
20	52.09	0.80	16.75	9.57	0.15	4.25	8.66	3.09	0.67	0.14	0.09	0.19	96.43	75
21	52.26	1.10	17.12	10.01	0.22	3.62	8.04	3.86	0.97	0.16	0.10	0.14	97.60	74
22	52.28	1.07	16.54	9.78	0.18	3.98	7.45	3.39	0.87	0.21	0.10	0.15	95.99	75
23	52.46	1.03	17.82	7.47	0.13	4.45	8.97	3.18	0.73	0.16	0.10	0.15	96.65	81
24	52.56	1.13	17.00	9.62	0.17	3.47	7.98	3.79	0.89	0.21	0.10	0.10	97.04	73
25	52.62	1.07	17.01	10.63	0.20	3.32	7.78	3.85	0.95	0.18	0.11	0.13	97.86	74
26	52.75	1.09	16.45	10.18	0.16	3.48	7.71	3.81	0.95	0.23	0.11	0.12	97.04	73
27	52.83	1.14	17.07	9.84	0.23	3.27	8.14	3.59	0.92	0.20	0.10	0.14	97.48	74
28	52.84	1.02	16.92	9.27	0.18	3.83	8.08	3.34	0.79	0.23	0.09	0.14	96.73	75
29	52.86	1.04	16.45	9.99	0.18	3.68	7.58	3.74	0.95	0.21	0.10	0.16	96.93	75
30	52.98	1.06	16.80	9.67	0.20	3.86	7.57	3.28	0.85	0.20	0.09	0.14	96.69	75
31	53.07	0.96	17.03	9.24	0.18	3.57	7.88	3.13	0.87	0.22	0.10	0.11	96.36	75
32	53.10	0.82	16.99	9.63	0.20	3.91	7.49	3.36	0.89	0.18	0.09	0.13	96.79	75
33	53.11	1.06	17.33	9.37	0.21	3.62	8.39	3.65	0.88	0.18	0.10	0.11	98.03	76
34	53.17	1.03	16.66	9.41	0.24	3.92	8.12	3.05	0.74	0.18	0.10	0.14	96.78	76

Table 4. (Contd.)

Inclusion no.	Component												Total	*Fo*
	SiO_2	TiO_2	Al_2O_3	FeO	MnO	MgO	CaO	Na_2O	K_2O	P_2O_5	Cl	S		
35	53.23	0.77	16.52	9.40	0.18	3.81	7.60	3.22	0.82	0.20	0.10	0.14	95.98	74
36	53.23	0.93	16.79	9.68	0.19	3.87	7.60	3.30	0.87	0.22	0.09	0.13	96.90	75
37	53.25	0.98	16.91	9.52	0.14	3.25	8.43	3.06	0.78	0.20	0.10	0.12	96.74	76
38	53.36	1.15	16.91	9.97	0.23	3.63	7.90	3.72	0.92	0.19	0.10	0.15	98.22	74
39	53.43	1.10	16.82	9.85	0.20	3.33	7.63	3.61	0.98	0.16	0.11	0.15	97.36	75
40	53.50	0.98	16.84	9.61	0.24	3.88	7.40	3.19	0.90	0.22	0.09	0.13	96.97	75
41	53.61	1.01	16.90	9.31	0.15	3.85	7.63	3.42	0.82	0.18	0.09	0.15	97.11	75
42	53.83	0.98	16.70	8.99	0.18	3.48	7.69	3.16	0.89	0.24	0.08	0.12	96.34	75
43	53.86	1.11	16.98	9.13	0.20	3.96	7.92	3.18	0.88	0.17	0.09	0.13	97.62	76
44	53.87	1.17	16.95	9.65	0.19	3.27	7.73	3.66	0.97	0.19	0.10	0.14	97.88	74
45	54.05	1.05	16.51	9.94	0.15	3.86	7.21	3.34	0.90	0.20	0.10	0.14	97.45	74
45	54.33	1.00	16.87	8.41	0.21	3.65	7.30	3.63	0.96	0.24	0.10	0.12	96.82	76
47	54.33	1.07	16.41	9.17	0.19	3.84	7.15	3.28	0.91	0.22	0.10	0.14	96.80	74
48	54.38	1.13	16.22	9.20	0.17	3.82	7.01	3.20	0.93	0.23	0.10	0.13	96.50	74
49	54.51	1.09	16.17	9.48	0.16	3.41	6.99	3.17	0.98	0.19	0.10	0.15	96.41	74
50	54.94	1.14	16.46	9.64	0.18	2.66	6.43	4.01	1.38	0.30	0.13	0.04	97.31	72
51	55.15	1.03	16.71	8.24	0.17	3.42	7.09	3.50	1.08	0.24	0.09	0.13	96.86	74
52	55.34	0.98	16.55	8.57	0.14	3.48	7.18	3.15	1.04	0.22	0.10	0.12	96.85	76
53	55.39	1.09	16.82	9.28	0.16	3.21	7.86	3.87	1.02	0.20	0.12	0.04	99.06	74
54	55.42	1.03	17.81	6.54	0.05	1.90	8.19	3.33	0.99	0.22	0.11	0.13	95.72	77
55	55.59	1.07	16.91	8.76	0.16	2.59	7.20	2.99	1.01	0.23	0.10	0.13	96.73	72
56	56.02	1.47	15.61	10.19	0.20	2.85	7.05	3.60	1.16	0.25	0.12	0.06	98.59	75
57	56.25	1.33	15.96	10.25	0.09	2.16	6.15	4.19	1.17	0.22	0.12	0.01	97.90	73
58	57.65	1.40	15.65	10.00	0.13	2.55	6.04	3.97	1.46	0.32	0.15	0.04	99.36	72
59	58.42	1.38	14.96	9.35	0.06	2.54	6.02	3.88	1.50	0.28	0.14	0.02	98.54	72

Table 5. Chemical composition (wt %) of glass in melt inclusions in olivine from basalt (sample KR99/96) from the Karymsky volcanic center

Inclusion no.	Component												Total	*Fo*
	SiO_2	TiO_2	Al_2O_3	FeO	MnO	MgO	CaO	Na_2O	K_2O	P_2O_5	Cl	S		
1	49.13	0.91	16.91	10.46	0.21	4.53	9.45	2.97	0.54	0.16	0.08	0.14	95.47	76
2	49.31	0.91	18.62	9.27	0.16	4.65	9.37	3.16	0.66	0.09	0.10	0.16	96.47	82
3	50.11	1.06	17.04	10.18	0.16	3.72	8.88	3.16	0.71	0.21	0.10	0.16	95.46	77
4	50.22	0.97	16.97	11.01	0.21	4.11	8.27	3.28	0.71	0.16	0.09	0.13	96.12	74
5	50.39	1.16	18.00	8.28	0.15	4.66	9.28	3.04	0.66	0.14	0.08	0.12	95.95	81
6	50.40	0.95	17.24	8.57	0.14	4.41	10.32	2.77	0.46	0.12	0.09	0.13	95.59	81
7	50.55	1.00	18.09	8.33	0.20	3.14	10.27	2.98	0.58	0.21	0.09	0.15	95.59	81
8	50.92	1.02	16.38	10.68	0.19	3.92	7.77	3.03	0.73	0.21	0.11	0.13	95.07	74
9	51.63	1.13	16.76	10.46	0.19	3.26	8.56	3.56	0.82	0.23	0.10	0.11	96.81	75
10	51.73	0.82	16.65	9.96	0.19	4.53	8.46	3.10	0.71	0.16	0.10	0.14	96.54	75
11	51.76	1.13	16.19	10.45	0.20	4.26	7.55	3.14	0.78	0.20	0.09	0.12	95.87	74
12	51.99	1.06	16.70	10.44	0.15	4.02	8.11	3.45	0.81	0.22	0.10	0.14	97.19	74
13	52.06	0.81	19.19	7.63	0.14	2.20	9.77	3.14	0.67	0.15	0.10	0.16	96.02	80
14	52.08	0.96	16.21	9.41	0.15	3.76	7.77	3.16	0.81	0.20	0.09	0.14	94.73	75
15	52.08	1.10	16.72	9.58	0.20	3.92	8.01	3.53	0.88	0.19	0.09	0.13	96.43	74
16	52.15	1.04	16.82	9.49	0.19	4.15	7.64	3.52	0.85	0.15	0.09	0.15	96.24	76
17	52.16	1.01	16.56	9.85	0.18	4.08	8.56	3.51	0.87	0.16	0.09	0.14	97.16	75
18	52.20	1.01	16.86	9.52	0.17	3.91	8.67	3.55	0.80	0.17	0.09	0.14	97.09	76
19	52.20	1.03	16.68	9.41	0.19	3.82	7.99	2.99	0.76	0.20	0.09	0.14	95.49	76
20	52.34	1.03	17.27	9.65	0.20	3.87	8.60	3.57	0.84	0.16	0.09	0.14	97.76	77
21	52.42	1.01	16.61	9.73	0.18	4.00	8.41	3.09	0.75	0.15	0.10	0.15	96.59	76
22	52.47	1.01	16.05	9.53	0.13	3.94	7.14	3.73	0.92	0.14	0.10	0.11	95.27	75
23	53.20	1.07	17.36	10.33	0.18	3.31	8.34	3.84	0.96	0.15	0.11	0.11	98.96	76
24	53.25	1.09	17.32	9.81	0.24	3.31	8.12	3.85	0.89	0.18	0.10	0.09	98.26	75
25	53.35	1.02	15.89	9.62	0.18	3.85	6.94	3.53	0.95	0.20	0.10	0.11	95.75	74
26	53.49	1.03	16.33	8.61	0.15	3.78	8.04	3.44	0.92	0.18	0.09	0.11	96.17	77
27	53.57	1.01	16.63	9.45	0.23	3.31	8.17	3.04	0.77	0.17	0.10	0.14	96.59	75
28	53.72	1.02	16.64	10.43	0.22	3.63	8.47	3.10	0.70	0.17	0.10	0.13	97.32	75
29	53.74	1.20	16.37	10.69	0.16	3.37	8.21	3.80	1.00	0.18	0.11	0.07	97.90	75
30	53.84	1.05	16.74	7.49	0.12	3.26	8.50	3.22	0.86	0.17	0.09	0.12	95.45	82
31	53.87	1.09	16.47	9.04	0.16	2.80	7.64	3.35	0.94	0.21	0.12	0.12	95.81	76
32	54.27	0.98	16.38	8.82	0.15	3.73	7.27	3.44	0.91	0.18	0.10	0.12	96.34	76
33	54.33	0.97	16.61	8.87	0.14	3.36	7.56	3.29	0.95	0.22	0.10	0.13	96.53	75
34	54.36	1.11	16.92	8.42	0.17	1.73	7.91	3.40	0.95	0.26	0.10	0.12	95.44	74
35	54.42	1.05	16.64	7.32	0.12	3.44	7.97	3.12	0.87	0.20	0.10	0.14	95.40	81
36	54.58	1.27	15.63	10.27	0.25	3.40	7.34	3.48	1.03	0.20	0.11	0.02	97.57	76
37	54.59	1.42	15.13	11.14	0.19	2.99	7.56	3.64	1.15	0.22	0.14	0.01	98.18	81
38	54.86	1.03	16.32	7.23	0.12	3.55	8.15	3.10	0.86	0.21	0.09	0.11	95.64	81

Table 6. Chemical composition (wt %) of glass in melt inclusions in plagioclase and pyroxene from basalt (sample KR96BV) from the Karymsky volcanic center

Inclusion no.	Component												Total	*An*, *Mg*#
	SiO_2	TiO_2	Al_2O_3	FeO	MnO	MgO	CaO	Na_2O	K_2O	P_2O_5	Cl	S		
Plagioclase														
1	51.64	0.98	16.95	9.95	0.18	4.71	8.45	3.47	0.63	0.13	0.09	0.14	97.32	89
2	51.69	1.19	16.49	10.84	0.24	4.03	7.47	3.52	0.83	0.14	0.14	0.19	96.77	81
3	52.09	1.08	16.57	9.84	0.18	4.07	8.09	3.62	0.76	0.11	0.07	0.13	96.61	89
4	52.44	1.13	17.06	8.81	0.15	3.91	7.97	3.74	0.94	0.17	0.09	0.14	96.55	83
5	52.47	0.93	16.59	8.72	0.15	4.76	8.31	3.31	0.67	0.16	0.09	0.12	96.28	83
6	52.60	1.11	16.68	10.28	0.23	3.70	7.23	3.34	0.99	0.11	0.10	0.12	96.49	81
7	52.72	1.05	16.12	9.37	0.19	3.89	7.53	4.17	0.95	0.16	0.09	0.15	96.39	85
8	52.77	1.07	16.57	9.19	0.22	3.87	7.93	3.81	0.99	0.19	0.07	0.14	96.82	83
9	52.77	1.11	15.69	10.93	0.22	3.96	6.72	3.67	1.12	0.09	0.15	0.15	96.58	81
10	52.93	1.08	16.34	8.95	0.22	3.86	7.88	3.68	0.95	0.17	0.09	0.15	96.30	83
11	53.09	1.09	16.42	9.22	0.20	3.98	7.69	3.76	0.96	0.20	0.09	0.16	96.86	85
12	53.10	1.11	16.71	8.92	0.20	3.48	7.76	3.70	0.82	0.07	0.08	0.15	96.10	88
13	53.10	1.14	15.62	10.03	0.21	4.32	7.20	3.52	0.97	0.22	0.14	0.13	96.60	73
14	53.21	0.93	16.24	10.09	0.16	3.58	6.65	3.77	1.16	0.09	0.10	0.11	96.09	83
15	53.31	1.15	17.12	8.63	0.21	3.64	7.71	3.70	0.91	0.17	0.06	0.15	96.76	79
16	53.37	1.04	16.82	8.80	0.17	3.76	7.59	3.36	0.91	0.22	0.07	0.13	96.24	85
17	53.40	1.05	16.78	8.71	0.16	3.92	7.84	3.52	0.93	0.12	0.08	0.15	96.66	83
18	53.65	1.07	17.14	8.63	0.16	3.63	7.56	3.79	0.93	0.20	0.06	0.13	96.95	79
19	53.65	1.22	15.48	10.26	0.22	4.48	7.46	3.58	0.91	0.13	0.10	0.17	97.66	83
20	53.74	1.10	15.86	10.43	0.21	3.49	6.28	3.93	1.26	0.16	0.16	0.14	96.76	81
21	53.81	1.19	16.53	8.81	0.16	3.62	7.41	3.83	0.94	0.14	0.07	0.15	96.66	79
22	53.90	1.08	16.27	9.76	0.19	3.52	6.80	3.90	1.04	0.08	0.07	0.16	96.77	81
23	53.98	1.17	16.60	8.28	0.17	3.05	6.87	4.51	1.15	0.18	0.09	0.18	96.23	89
24	54.00	0.87	17.08	8.90	0.17	3.45	7.53	3.35	0.83	0.12	0.11	0.12	96.53	89
25	54.07	1.10	16.71	8.70	0.20	4.06	7.19	3.50	0.91	0.15	0.11	0.13	96.83	87
26	54.10	1.15	16.46	8.66	0.16	3.54	7.09	3.72	0.99	0.06	0.13	0.14	96.20	86
27	54.13	1.18	15.08	9.81	0.20	4.51	6.64	3.19	1.07	0.10	0.12	0.14	96.07	73
28	54.16	1.03	16.57	8.47	0.15	3.58	7.08	3.84	1.02	0.07	0.10	0.14	96.21	86
29	54.16	1.40	11.89	13.05	0.27	6.23	6.62	3.16	1.17	0.15	0.15	0.07	98.32	73
30	54.49	1.15	16.47	8.95	0.19	3.78	7.44	3.95	1.02	0.15	0.08	0.07	97.74	88

Table 6. (Contd.)

Inclusion no.	Component												Сумма	*An*, *Mg*#
	SiO_2	TiO_2	Al_2O_3	FeO	MnO	MgO	CaO	Na_2O	K_2O	P_2O_5	Cl	S		
31	54.56	1.16	15.28	9.38	0.17	3.90	6.90	4.23	1.02	0.15	0.13	0.14	97.02	88
32	54.60	0.62	16.74	8.15	0.18	3.84	6.98	3.80	1.07	0.01	0.10	0.05	96.14	86
33	54.84	0.84	17.27	8.12	0.20	3.33	7.36	3.42	0.85	0.03	0.10	0.13	96.49	89
34	55.01	1.13	16.54	7.79	0.14	2.91	6.81	3.97	1.23	0.21	0.08	0.17	95.99	83
35	55.02	1.08	17.05	7.81	0.18	3.20	7.39	3.44	1.01	0.25	0.08	0.12	96.63	83
36	55.36	1.36	14.11	10.68	0.24	3.94	6.19	3.90	1.17	0.22	0.13	0.02	97.32	88
37	55.41	1.08	16.96	8.15	0.21	3.16	6.85	3.98	1.21	0.18	0.08	0.13	97.40	87
38	56.39	0.97	16.75	7.76	0.19	2.80	5.95	4.21	1.37	0.13	0.10	0.13	96.75	79
Pyroxene														
39	51.92	1.10	16.89	9.53	0.21	3.79	7.90	4.05	0.82	0.08	0.08	0.16	96.53	80
40	51.98	1.10	16.81	10.02	0.18	4.06	8.23	3.16	0.68	0.06	0.07	0.15	96.50	77
41	51.99	1.05	16.69	9.27	0.17	4.06	8.23	3.89	0.80	0.08	0.08	0.16	96.47	80
42	52.00	1.12	17.24	10.28	0.22	3.92	8.16	3.86	0.81	0.03	0.06	0.14	97.84	80
43	52.27	1.13	17.40	10.56	0.19	3.68	7.76	3.96	0.86	0.03	0.10	0.16	98.10	80
44	52.45	1.14	16.03	9.45	0.19	4.11	8.27	3.42	0.70	0.06	0.08	0.16	96.06	77
45	52.66	1.16	16.07	9.57	0.21	4.00	8.15	3.60	0.81	0.07	0.07	0.18	96.55	77
46	53.26	1.12	17.44	9.67	0.23	3.46	7.71	3.92	0.88	0.17	0.10	0.15	98.11	76
47	53.48	1.20	17.17	8.67	0.19	3.49	7.74	3.77	1.00	0.09	0.10	0.17	97.07	77
48	54.19	1.15	15.83	9.24	0.21	3.72	7.63	3.64	0.79	0.32	0.10	0.15	96.97	73
49	54.27	1.19	15.62	9.25	0.21	3.69	6.95	4.10	1.02	0.38	0.11	0.14	96.93	73
50	54.62	1.29	16.01	9.43	0.19	3.27	7.23	3.60	0.99	0.20	0.08	0.12	97.03	77
51	55.76	1.24	16.46	9.78	0.16	3.17	6.64	4.12	1.09	0.14	0.05	0.05	98.66	80
52	58.60	1.04	15.17	7.33	0.17	2.62	5.91	3.77	1.40	0.11	0.11	0.04	96.27	77

Table 7. Chemical composition (wt %) of glass in melt inclusions in plagioclase and pyroxene from basalt (sample KR99/96) from the Karymsky volcanic center

Inclusion no.	Component												Total	*An*, *Mg*#
	SiO_2	TiO_2	Al_2O_3	FeO	MnO	MgO	CaO	Na_2O	K_2O	P_2O_5	Cl	S		
Plagioclase														
1	50.40	1.04	16.55	9.59	0.18	4.25	8.45	3.70	0.74	0.11	0.10	0.19	95.30	90
2	51.55	1.15	14.83	10.90	0.25	4.75	8.50	4.04	0.96	0.19	0.10	0.16	97.38	87
3	51.72	1.31	13.94	11.89	0.27	5.32	7.87	3.80	1.20	0.14	0.13	0.12	97.71	84
4	52.13	1.33	13.51	12.39	0.30	5.21	7.80	3.32	1.06	0.10	0.12	0.16	97.43	81
5	52.25	1.12	16.02	9.01	0.17	5.13	7.84	3.69	0.73	0.20	0.12	0.15	96.43	89
6	52.27	1.21	15.69	10.48	0.22	3.83	7.47	3.46	0.81	0.15	0.20	0.15	95.94	86
7	52.40	1.39	13.44	12.16	0.23	5.52	7.41	3.80	0.99	0.17	0.10	0.16	97.7	85
8	53.23	1.16	15.80	9.98	0.19	4.15	7.89	3.43	0.94	0.03	0.16	0.14	97.10	90
9	53.27	1.21	16.00	9.45	0.20	4.68	7.50	3.69	0.92	0.12	0.11	0.23	97.38	92
10	53.32	1.13	15.83	9.79	0.22	4.37	7.89	3.67	1.03	0.02	0.08	0.14	97.49	85
11	53.35	1.03	16.52	8.62	0.17	3.64	7.73	3.77	0.93	0.12	0.06	0.13	96.07	85
12	53.39	1.21	16.58	8.32	0.17	3.43	8.10	3.31	0.89	0.04	0.08	0.18	95.70	88
13	53.41	1.18	13.57	12.06	0.24	5.52	7.39	3.86	0.96	0.07	0.09	0.11	98.46	84
14	53.54	1.08	16.60	8.48	0.14	3.63	8.04	3.68	0.99	0.23	0.06	0.12	96.59	87
15	53.58	1.24	15.85	10.63	0.23	3.71	7.04	3.59	1.05	0.19	0.13	0.16	97.40	88
16	53.71	1.39	13.42	11.45	0.22	5.06	7.03	3.44	1.18	0.17	0.09	0.12	97.28	92
17	53.73	1.19	16.59	9.48	0.17	3.47	7.76	3.89	0.82	0.26	0.08	0.15	97.59	85
18	53.74	1.07	17.06	9.10	0.25	3.16	7.64	3.70	1.09	0.09	0.10	0.14	97.14	89
19	53.79	1.06	16.79	8.93	0.20	3.81	7.82	3.95	0.97	0.13	0.07	0.16	97.68	85
20	53.99	1.02	16.75	7.77	0.14	3.46	7.67	3.55	0.87	0.13	0.06	0.13	96.54	82
21	54.10	1.46	12.93	11.45	0.22	5.28	6.85	3.69	1.20	0.33	0.10	0.04	97.65	92
22	54.23	1.05	16.98	8.22	0.15	3.20	7.65	3.49	0.92	0.15	0.07	0.29	96.40	86
23	54.27	1.08	16.24	8.60	0.19	3.89	7.94	3.53	0.96	0.14	0.09	0.19	97.12	90
24	54.29	1.44	13.44	11.83	0.17	4.79	7.20	3.54	1.03	0.27	0.18	0.10	98.28	85
25	54.36	1.17	16.48	8.50	0.18	3.78	7.67	4.26	0.90	0.14	0.11	0.16	97.71	82
26	54.46	1.21	15.74	8.50	0.20	3.25	7.23	3.51	1.11	0.12	0.05	0.17	95.55	83
27	54.65	1.22	17.18	8.20	0.21	3.13	7.10	3.48	0.99	0.12	0.08	0.30	96.66	85
28	54.68	1.06	16.88	8.16	0.22	3.84	8.10	3.63	0.82	0.18	0.11	0.17	97.85	84
29	54.75	1.09	16.18	8.44	0.13	3.85	8.19	3.39	0.90	0.14	0.04	0.18	97.28	80
30	54.91	0.98	16.50	8.03	0.17	3.45	7.18	3.68	1.08	0.18	0.07	0.13	96.36	82

Table 7. (Contd.)

Inclusion no.	Component												Total	*An*, *Mg*#
	SiO_2	TiO_2	Al_2O_3	FeO	MnO	MgO	CaO	Na_2O	K_2O	P_2O_5	Cl	S		
31	55.00	1.21	14.89	10.23	0.21	3.80	6.62	4.24	1.26	0.20	0.08	0.14	97.88	88
32	55.16	1.37	13.54	11.22	0.23	4.97	6.91	3.67	1.12	0.18	0.12	0.05	98.54	88
33	55.21	1.09	16.74	8.26	0.19	3.24	7.30	3.72	1.14	0.12	0.08	0.15	97.24	81
34	55.26	1.15	15.10	8.70	0.18	3.92	6.88	3.42	1.22	0.15	0.09	0.14	96.21	85
35	55.30	0.89	16.91	8.11	0.16	3.77	7.63	3.53	0.88	0.08	0.08	0.10	97.44	81
36	55.50	1.43	13.61	11.20	0.19	4.78	6.72	3.26	1.14	0.24	0.09	0.03	98.19	88
37	55.52	1.24	15.48	8.63	0.21	3.70	6.95	3.93	1.17	0.12	0.12	0.16	97.43	83
38	55.56	1.00	16.29	8.02	0.11	3.39	7.35	3.78	0.96	0.16	0.13	0.11	96.86	89
39	55.73	1.11	17.09	6.89	0.16	2.65	7.19	3.72	1.13	0.11	0.04	0.13	95.95	85
40	55.80	1.48	14.02	10.74	0.21	4.35	6.49	3.87	1.18	0.26	0.08	0.02	98.50	85
41	55.85	1.17	15.53	8.72	0.21	3.17	5.99	3.77	1.47	0.16	0.10	0.14	96.28	79
42	55.86	1.38	13.81	10.32	0.21	4.55	6.83	3.70	1.14	0.29	0.13	0.04	98.26	82
43	56.04	1.16	16.14	8.71	0.16	3.74	6.76	3.47	1.29	0.13	0.11	0.15	97.86	83
44	56.43	1.03	16.87	7.22	0.18	2.80	6.31	4.10	1.45	0.26	0.09	0.13	96.87	82
45	56.63	1.02	17.35	7.16	0.17	2.51	6.23	4.18	1.32	0.12	0.11	0.09	96.89	81
46	56.72	0.98	15.80	7.67	0.13	3.25	6.95	3.62	1.02	0.28	0.07	0.08	96.57	88
47	57.17	1.27	15.06	9.23	0.21	3.48	6.20	4.22	1.34	0.27	0.09	0.03	98.57	80
48	58.75	1.28	13.20	8.65	0.21	3.35	5.21	3.38	1.83	0.15	0.17	0.30	96.48	79
							Pyroxene							
49	53.33	1.10	15.60	10.01	0.17	3.76	7.51	3.39	0.72	0.21	0.08	0.15	96.03	77
50	53.62	1.08	16.17	9.71	0.22	3.77	7.29	3.09	0.74	0.21	0.10	0.12	96.12	77
51	54.07	1.19	15.96	10.39	0.16	3.56	7.31	3.35	0.68	0.13	0.13	0.12	97.05	77
52	54.64	1.08	16.35	8.93	0.25	3.66	7.63	3.68	0.84	0.16	0.07	0.16	97.45	78
53	55.16	1.18	16.20	9.07	0.26	3.19	6.59	3.45	0.90	0.25	0.08	0.16	96.49	77
54	55.42	1.16	16.29	9.25	0.19	3.15	6.98	3.98	1.08	0.20	0.07	0.04	97.81	78
55	56.54	1.02	14.74	8.82	0.15	3.30	7.21	3.65	0.91	0.13	0.07	0.18	96.72	73
56	56.98	1.18	14.95	9.30	0.17	3.22	6.91	3.13	0.96	0.11	0.11	0.15	97.17	73
57	57.23	1.02	14.43	9.41	0.24	3.06	6.83	3.12	0.84	0.19	0.13	0.17	96.67	73
58	57.62	1.12	14.91	8.64	0.22	3.09	6.27	3.62	0.92	0.26	0.08	0.13	96.88	76
59	57.81	1.26	14.65	8.25	0.18	3.15	6.46	3.58	0.93	0.30	0.11	0.14	96.82	76

Table 8. Average composition (wt %) of the rocks, parental melt, melt inclusions in olivine (*Ol*), clinopyroxene (*Cpx*), and plagioclase (*Pl*), and matrix glass

Component	Basalt		Parental melt		Melt inclusions in *Ol*		Melt inclusions in *Cpx*		Melt inclusions in *Pl*		Matrix glass		Andesite	
	Average	1s	Average	1s	Average	1s	Average	1s	Average	1s	Average	1s	Average	1s
	$n = 5$		$n = 5$		$n = 92$		$n = 25$		$n = 87$		$n = 2$		$n = 2$	
SiO_2	51.78	*0.16*	50.22	*0.56*	53.22	*1.48*	54.86	*2.10*	54.51	*1.42*	58.20	*0.36*	62.21	*0.42*
TiO_2	0.73	*0.01*	0.90	*0.02*	1.02	*0.10*	1.15	*0.07*	1.15	*0.15*	1.40	*0.01*	0.89	*0.02*
Al_2O_3	19.15	*0.11*	17.04	*0.33*	16.25	*0.51*	16.17	*0.88*	16.02	*1.24*	15.07	*0.34*	16.29	*0.52*
FeO	7.66	*0.32*	9.91	*0.60*	9.55	*0.79*	9.43	*0.70*	9.40	*1.30*	9.52	*0.32*	5.85	*0.48*
MnO	0.15	*0.00*	0.15	*0.04*	0.18	*0.04*	0.20	*0.03*	0.19	*0.03*	0.09	*0.03*	0.15	*0.01*
MgO	5.49	*0.18*	5.59	*0.83*	4.44	*0.57*	3.55	*0.38*	3.93	*0.70*	2.57	*0.01*	1.93	*0.09*
CaO	10.56	*0.09*	9.43	*0.59*	8.01	*0.74*	7.40	*0.66*	7.35	*0.63*	6.08	*0.01*	5.22	*0.24*
Na_2O	2.86	*0.03*	2.98	*0.14*	3.31	*0.27*	3.67	*0.31*	3.73	*0.27*	3.96	*0.05*	4.52	*0.18*
K_2O	0.58	*0.01*	0.56	*0.09*	0.82	*0.14*	0.89	*0.16*	1.04	*0.19*	1.50	*0.02*	1.61	*0.05*
P_2O_5	0.14	*0.00*	0.13	*0.03*	0.18	*0.04*	0.17	*0.10*	0.15	*0.06*	0.30	*0.02*	0.25	*0.01*
H_2O	–	–	2.81	*0.45*	2.79	*0.67*	2.29	*0.27*	2.29	*0.29*	1.14	*0.02*	–	–
S	–	–	0.20	*0.03*	0.13	*0.03*	0.09	*0.04*	0.10	*0.05*	0.03	*0.01*	–	–
Cl	–	–	0.084	*0.013*	0.10	*0.01*	0.13	*0.02*	0.14	*0.03*	0.14	*0.01*	–	–
Total	99.10		100.00		100.00		100.00		100.00		100.00		98.91	
T (°C)			1062		1047		1035		1052		1044			

Note: the liquidus temperature was calculated by the model [21] with regard of water content in the melt [22]. The average compositions of basalt of the 1996 eruption and andesite of the 1963–1999 eruptions of Karymsky volcano are according to [4].

The exception is Li, whose concentration in inclusions in plagioclase (13–31 ppm) is systematically higher than in inclusions in pyroxene and olivine (5–10 ppm). The primitive mantle-normalized Li concentrations in the matrix glass and inclusions in the pyroxene and olivine are close to the concentrations of HREE and Y or are more deficient ($Li_N/Y_N = 0.3–1.3$). Inclusions in plagioclase are strongly enriched in this element ($Li_N/Y_N = 2.1–4.7$) relative to REE and Y. The compositions of inclusions in plagioclase in basalts of the 1996 eruption published in [6] show a distribution of trace elements similar to those of our inclusions but differ from the latter in being even more strongly enriched in Li (Li = 118–284 ppm, $Li_N/Y_N = 16–50$) (Fig. 6d).

DISCUSSION

Distinctive features of melt crystallization. The composition of the parental, the most primitive melt was evaluated by averaging the compositions of melt inclusions with $SiO_2 < 52.5$ wt % in olivine (Fig. 8). The concentrations of volatile components of the melts were calculated proceeding from the maximum volatile/K_2O ratios of all of our inclusions (Fig. 4). The parental melt had a high-Al low-Mg basaltic composition and was in equilibrium with olivine of the composition Fo_{80} at a temperature of 1062°C. The pressure of crystallization onset was estimated at approximately 1.5 kbar (a depth of approximately 5 km) based on the maximum measured H_2O concentration (close to 3.9 wt %) in the melt inclusions [24]. The H_2O concentration of the residual melt (~1.1 wt %) corresponds to latest stages crystallization at a pressure of approximately 100 bar.

The parental melt evolved during the simultaneous crystallization of olivine, clinopyroxene, plagioclase, and magnetite, as follows from petrographic relations of these minerals in the rocks (Fig. 2) and from the similar compositions of melt inclusions in various minerals (Fig. 4, Table 8). These results provide further support for the previously established fact of the similar composition of melt inclusions in the simultaneously crystallizing minerals [25] and, hence, the absence of any sig-

Table 9. Chemical composition (wt %) of melt inclusions in olivine from basalt of the 1996 eruption

Component	Sample KR96BV				Sample KR99/96		
SiO_2	51.13	50.01	54.82	55.36	51.28	51.42	52.88
TiO_2	1.00	0.88	1.13	1.09	0.95	1.16	1.01
Al_2O_3	18.57	17.40	15.84	15.79	16.83	17.58	16.22
FeO	9.75	8.88	8.97	9.25	8.36	8.07	9.49
MnO	0.16	0.11	0.17	0.16	0.14	0.15	0.18
MgO	3.81	4.89	3.82	3.41	4.41	4.66	4.00
CaO	9.63	10.23	7.01	6.99	10.32	9.28	8.41
Na_2O	3.51	2.84	3.20	3.17	2.77	3.04	3.09
K_2O	0.73	0.44	0.93	0.98	0.46	0.66	0.75
P_2O_5	0.14	0.14	0.23	0.19	0.12	0.14	0.15
F	0.034	0.015	0.034	0.029	0.022	0.026	0.030
Cl	0.10	0.08	0.10	0.10	0.09	0.08	0.10
S	0.14	0.14	0.13	0.15	0.13	0.12	0.15
H_2O	1.56	2.80	3.15	3.03	2.71	2.92	2.63
Total	100.26	98.86	99.53	99.70	98.59	99.31	99.09
Fo	82	80	74	74	81	81	76

nificant influence of boundary effects on the composition of melt inclusions in minerals in the basalts.

Our mass-balance calculations (Table 12) indicate that the degree of crystallization of the parental melt at the time of its eruption was close to 55%. The predominant crystallizing phase was plagioclase (33.5%), with olivine, clinopyroxene, and magnetite crystallizing in subordinate amounts (7.2, 9.7, and 3.5%, respectively). The crystallization of the melt was associated with its degassing, as follows from the decrease in the H_2O and S concentrations of the melts and from the decrease in the volatile/K_2O ratios at increasing degree of melt crystallization (Fig. 5). The evaluated amount of water-rich fluid (~92 wt % H_2O) that separated from the melt in the course of its crystallization was 2.5% (Table 12). At a density of the fluid phase of ~0.1 g/cm^3, this fluid amount corresponds to approximately 25 vol % of the erupted magma, which is close to the measured porosity of the rocks (20–40%).

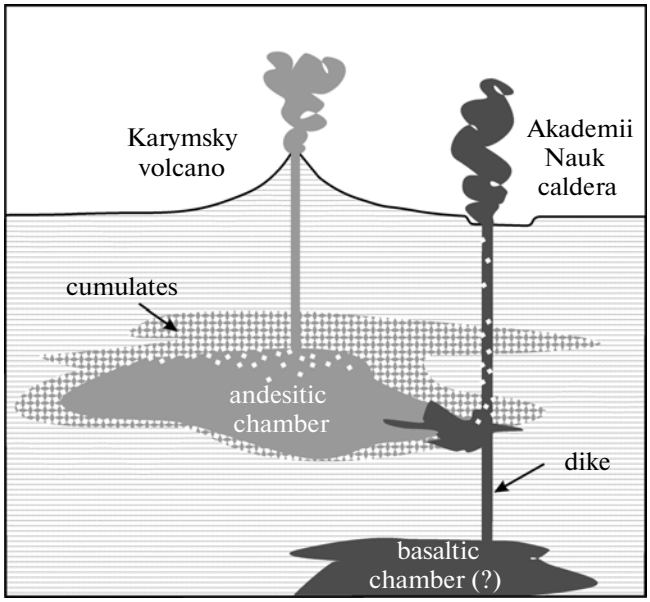

Fig. 7. Hypothetical scenario of the 1996 eruption at the Karymsky volcanic center. The basaltic eruption in the Akademii Nauk caldera is thought to be a magma breakthrough from a deep-sitting chamber. The magma entrained fragments of plagioclase cumulates from the apical part of a shallow-sitting andesite chamber.

Inasmuch as H_2O concentrations in magmas at an H_2O activity in the fluid close to unity is controlled mostly by the equilibrium pressure, a decrease in the H_2O concentration during crystallization implies a decompressional regime of crystallization during magma ascent. As is shown in Fig. 8, the calculated liquidus temperature of the parental melt (1062°C), intermediate crystallization products (average compositions of the melt inclusions, 1035–1052°C), and the matrix melt (final crystallization product, 1044°C) are similar within the errors of the models (±20°C [21, 22]). Hence, a decrease in the temperature of the magma induced by its conductive cooling could not trigger the crystallization of minerals of the rocks. In this instance, crystallization was nearly isothermal and was caused by an increase in the activities of silicate components in the

Table 10. Chemical composition (major components in wt %, trace elements in ppm) of melt inclusions in olivine, clinopyroxene, and plagioclase from basalt of the 1996 eruption (sample KR96BV)

Component	1	2	3	4	5	6	7	8	9	10	11	12
	olivine					plagioclase				clinopyroxene		
SiO_2	52.58	53.80	53.72	55.34	56.77	52.44	52.77	52.77	53.65	51.66	53.26	53.48
TiO_2	1.32	1.01	1.03	1.10	1.07	1.13	1.07	1.11	1.07	1.16	1.12	1.20
Al_2O_3	16.35	16.57	17.41	16.43	16.51	17.06	16.57	15.69	17.14	16.07	17.44	17.17
FeO	9.92	8.64	7.29	9.61	8.55	8.81	9.19	10.93	8.63	9.57	9.67	8.67
MnO	0.19	0.21	0.13	0.20	0.16	0.15	0.22	0.22	0.16	0.21	0.23	0.19
MgO	4.38	4.29	4.45	3.33	2.59	3.91	3.87	3.96	3.63	4.00	3.46	3.49
CaO	8.06	8.03	8.97	7.63	7.20	7.97	7.93	6.72	7.56	8.15	7.71	7.74
Na_2O	3.26	3.24	3.18	3.61	2.99	3.74	3.81	3.67	3.79	3.60	3.92	3.77
K_2O	0.74	0.80	0.73	0.98	1.01	0.94	0.99	1.12	0.93	0.81	0.88	1.00
P_2O_5	0.21	0.21	0.16	0.16	0.23	0.17	0.19	0.09	0.20	0.07	0.17	0.19
Cl	0.09	0.09	0.10	0.11	0.10	0.09	0.07	0.15	0.06	0.07	0.10	0.10
S	0.14	0.14	0.15	0.15	0.13	0.14	0.14	0.15	0.13	0.18	0.15	0.17
H_2O	2.53	3.63	3.46	1.70	3.90	2.24	2.05	2.29	1.95	2.35	1.68	2.93
Total	99.77	100.66	100.78	100.38	101.24	98.79	98.87	98.87	98.90	97.90	99.79	100.10
Li	6.72	7.23	6.14	7.54	10.3	16.6	25.5	12.8	17.9	5.87	9.24	8.07
Be	0.60	0.72	0.74	0.55	0.85	0.62	0.56	0.64	0.58	0.61	0.70	0.69
B	8.13	8.10	7.9	7.74	10.6	8.47	7.41	6.85	8.18	7.35	8.95	8.82
F	315	296	228	453	354	318	632	401	302	400	288	389
V	475	308	307	294	290	270	399	379	293	317	321	279
Cr	125	53	70	134	21	46.5	42.1	49.9	33.1	37.4	22.9	27.8
Sr	439	413	429	324	392	377	354	361	377	373	400	382
Ba	265	261	229	229	316	247	213	237	236	215	237	288
Y	22.6	20.0	20.0	18.5	23.0	17.8	18.1	16.7	19.2	21.3	19.2	20.5
Zr	89.8	84.2	78.2	77.0	102	81.6	62.3	45.1	83.5	70.9	85.8	73.3
Nb	2.87	2.40	2.36	2.20	2.89	2.35	2.49	1.70	2.60	1.78	2.47	2.21
La	7.90	7.24	6.93	6.20	8.98	6.25	5.37	5.70	6.26	5.90	6.72	6.97
Ce	20.0	18.6	17.2	16.3	22.4	17.6	14.2	14.1	17.4	16.2	17.6	18.2
Nd	13.9	12.0	11.8	10.7	14.0	10.8	9.70	9.71	10.7	11.1	11.2	11.6
Sm	3.57	3.35	3.25	3.00	4.04	3.26	2.75	2.48	3.05	3.39	3.20	3.23
Eu	1.20	1.10	1.39	0.86	1.23	0.96	1.00	1.13	0.84	1.11	0.94	1.15
Gd	4.31	3.92	3.77	3.52	4.52	3.45	2.68	2.40	3.23	3.89	2.98	2.79
Dy	3.74	3.55	3.41	3.08	4.17	2.99	2.99	2.59	3.07	3.54	2.94	3.34
Er	2.69	2.60	2.39	2.19	2.91	2.11	2.05	1.71	2.21	2.52	2.31	2.32
Yb	2.48	2.49	2.40	1.88	2.69	1.95	2.06	1.54	2.01	2.49	2.10	2.22
Hf	2.47	2.60	2.25	2.10	3.05	2.08	1.95	1.52	2.38	2.06	2.39	2.12
Pb	3.41	3.60	2.65	2.17	3.86	3.01	2.92	3.59	3.15	2.95	3.71	3.66
Th	0.79	0.78	0.76	0.60	1.05	0.58	0.50	0.31	0.75	0.52	0.76	0.64
U	0.43	0.49	0.50	0.33	0.59	0.45	0.27	0.27	0.42	0.37	0.43	0.42

Table 11. Chemical composition (major components in wt %, trace elements in ppm) of melt inclusions in olivine, clinopyroxene, and plagioclase from basalt of the 1996 eruption (sample KR99/96)

Component	1	2	3	4	5	6	7	8	9	10	11	12
	olivine					clinopyroxene				plagioclase		
SiO_2	51.52	50.73	52.09	53.61	56.10	53.33	53.62	55.16	56.54	50.40	52.40	54.10
TiO_2	0.91	0.91	1.00	0.96	1.03	1.10	1.08	1.18	1.02	1.04	1.39	1.46
Al_2O_3	18.19	16.51	17.66	15.83	15.93	15.60	16.17	16.20	14.74	16.55	13.44	12.93
FeO	9.04	10.20	8.13	9.18	7.06	10.01	9.71	9.07	8.82	9.59	12.16	11.45
MnO	0.16	0.21	0.20	0.15	0.12	0.17	0.22	0.26	0.15	0.18	0.23	0.22
MgO	4.65	4.53	3.14	3.76	3.55	3.76	3.77	3.19	3.30	4.25	5.52	5.28
CaO	9.37	9.45	10.27	7.77	8.15	7.51	7.29	6.59	7.21	8.45	7.41	6.85
Na_2O	3.16	2.97	2.98	3.16	3.10	3.39	3.09	3.45	3.65	3.70	3.80	3.69
K_2O	0.66	0.54	0.58	0.81	0.86	0.72	0.74	0.90	0.91	0.74	0.99	1.20
P_2O_5	0.09	0.16	0.21	0.20	0.21	0.21	0.21	0.25	0.33	0.11	0.17	0.33
Cl	0.10	0.08	0.09	0.09	0.09	0.08	0.10	0.08	0.07	0.10	0.10	0.10
S	0.16	0.14	0.15	0.14	0.11	0.15	0.12	0.16	0.18	0.19	0.16	0.04
H_2O	2.66	2.22	2.60	3.68	3.86	2.65	2.55	2.44	2.17	2.10	2.51	2.78
Total	100.67	98.65	99.10	99.34	100.71	98.68	98.67	98.93	99.09	97.40	100.58	100.43
Li	7.06	5.98	4.82	8.01	5.14	7.01	7.03	6.33	6.19	24.8	30.8	24.9
Be	0.64	0.48	0.60	0.78	0.45	0.62	0.64	0.69	1.03	0.50	0.53	0.60
B	7.2	4.9	6.6	9.3	10.1	8.47	8.49	9.49	10.2	6.36	7.57	6.52
F	380	322	250	303	316	565	425	386	300	339	255	293
V	295	285	327	289	214	378	307	310	225	395	350	336
Cr	49	58	72	40	65	27.4	48.2	41.1	22.4	35.1	24.0	38.6
Sr	424	461	477	381	404	394	343	363	326	380	366	373
Ba	197	207	222	255	302	206	204	247	236	211	223	232
Y	16.0	18.9	21.0	21.0	21.4	17.2	22.1	19.8	49.5	18.0	17.6	15.7
Zr	55.5	66.1	78.1	85.6	105	64.1	80.6	87.9	118	58.3	65.8	43.1
Nb	1.74	2.10	2.44	2.47	3.24	1.97	2.24	2.61	2.29	2.22	1.94	1.54
La	5.65	6.00	7.93	7.42	8.70	5.42	6.05	6.96	8.53	5.55	5.41	5.18
Ce	14.7	16.0	20.2	18.8	22.4	15.5	17.2	18.9	29.2	14.2	15.2	13.7
Nd	10.2	11.2	13.6	12.7	14.0	9.77	11.0	11.2	23.8	9.90	10.0	8.68
Sm	2.62	3.19	3.84	3.31	4.04	2.54	3.31	2.94	7.48	2.53	2.82	2.58
Eu	1.04	1.16	1.22	1.22	1.29	0.87	1.02	1.06	1.25	0.99	0.90	1.03
Gd	3.46	3.55	4.38	3.75	4.29	2.35	3.50	3.26	6.93	2.55	2.94	2.28
Dy	2.82	3.30	3.93	3.64	3.86	2.66	3.45	2.95	7.95	2.71	2.93	2.58
Er	1.94	2.07	2.65	2.34	2.56	1.85	2.48	2.22	5.90	1.98	2.05	1.85
Yb	1.74	2.08	2.84	2.41	2.25	1.95	2.31	2.16	5.65	1.68	1.99	1.78
Hf	1.76	2.14	2.84	2.49	3.20	1.85	2.30	2.27	4.19	1.85	1.66	1.50
Pb	3.25	2.28	2.72	3.72	2.83	2.59	2.19	2.43	2.94	2.47	3.21	3.22
Th	0.51	0.52	0.71	0.75	0.93	0.46	0.59	0.82	0.65	0.43	0.56	0.34
U	0.25	0.32	0.58	0.49	0.59	0.33	0.44	0.58	0.45	0.30	0.26	0.25

Table 12. Mass-balance calculations for the compositions of the rock, parental melt, and residual melt

Composition	Mass proportion, %	Volume proportion, %	SiO_2	TiO_2	Al_2O_3	FeO*	MnO	MgO	CaO	Na_2O	K_2O	P_2O_5	H_2O	S	Cl	ΣX^2
Calculation 1: residual melt + minerals + fluid = parental melt																
residual melt	43.7	28.8	58.98	1.42	15.27	9.65	0.09	2.60	6.16	4.01	1.52	0.31	1.14	0.03	0.14	
olivine	7.2	3.6	38.05	–	–	22.26	0.28	38.64	0.19	–	–	–	–	–	–	
clinopyroxene	9.7	4.8	51.37	0.51	2.44	8.8	0.36	15.64	20.55	0.31	–	–	–	–	–	
plagioclase	33.5	21.2	50.82	0.12	29.98	1.04	0.00	0.16	14.10	3.49	0.15	–	–	–	–	
magnetite	3.5	1.1	0.32	10.78	4.02	81.19	0.27	2.98	0.12	–	–	–	–	–		
fluid	2.5	40.4	–	–	–	–	–	–	–	–	–	–	**91.7**	**7.4**	**0.8**	
result	100	–	**50.16**	**1.08**	**17.00**	**9.82**	**0.10**	**5.57**	**9.38**	**2.93**	**0.70**	**0.13**	**2.75**	**0.20**	**0.08**	
parental melt			**50.22**	**0.90**	**17.04**	**9.91**	**0.15**	**5.59**	**9.43**	**2.98**	**0.56**	**0.13**	**2.81**	**0.20**	**0.08**	
X^2			*0.005*	*0.034*	*0.002*	*0.008*	*0.002*	*0.001*	*0.002*	*0.003*	*0.020*	*0.000*	*0.004*	*0.000*	*0.000*	*0.081*
Calculation 2: residual melt + minerals = rock																
residual melt	34.9	37.6	58.98	1.42	15.27	9.65	0.09	2.60	6.16	4.01	1.52	0.31	–	–	–	
olivine	7.7	6.3	38.05	–	–	22.26	0.28	38.64	0.19	–	–	–	–	–	–	
clinopyroxene	10.3	8.4	51.37	0.51	2.44	8.8	0.36	15.64	20.55	0.31	–	–	–	–	–	
plagioclase	45.4	46.9	50.82	0.12	29.98	1.04	0.00	0.16	14.10	3.49	0.15	–	–	–	–	
magnetite	1.6	0.8	0.32	10.78	4.02	81.19	0.27	2.98	0.12	–	–	–	–	–	–	
result	100	–	**51.91**	**0.78**	**19.27**	**7.80**	**0.10**	**5.61**	**10.69**	**3.02**	**0.60**	**0.11**	–	–	–	
parental melt	–	–	**51.78**	**0.73**	**19.15**	**7.66**	**0.15**	**5.49**	**10.56**	**2.86**	**0.58**	**0.14**	–	–	–	
X^2			*0.018*	*0.002*	*0.015*	*0.020*	*0.003*	*0.014*	*0.015*	*0.025*	*0.000*	*0.001*	–	–	–	*0.114*

Note: the calculations were carried out by the Solver utility of the MS Excel application by minimizing the totals of squared errors (ΣX^2). The volume proportions of phases were calculated using their densities: 2.4 g cm^{-1} for basalt–andesite melt, 3.3 g cm^{-1} for olivine and pyroxene, 2.6 g cm^{-1} for plagioclase, 5.2 g cm^{-1} for magnetite, and 0.1 g cm^{-1} for fluid.

melt during H_2O degassing from it. With reference to Karymsky volcano, the lost of ~2.5% H_2O from the melts resulted in their ~55 % crystallization, which would be equivalent to a ~80°C temperature decrease during the crystallization of aluminous basalt in a closed system [26].

As follows from data recently obtained by several researchers [27–29], massive magma crystallization during its ascent, a process associated with magma degassing and the capture of numerous melt inclusions in minerals, is typical of island arcs. This is always caused by a high initial water concentration in the magmas and their practically complete degassing during eruption, which makes island arcs different from other geodynamic environments [30]. The compositions of most melt inclusions entrapped during this process correspond, as is the case with our inclusions and rocks, not to the crystallization of the magmas in the chambers but to the composition of the melts during their ascent immediately before their eruptions.

Relations between rock and melt compositions. The compositions of the parental melt and rocks erupted in 1996 are close in terms of concentrations of most major components (SiO_2, MgO, CaO, Na_2O, and K_2O). The differences between these compositions are the higher Al_2O_3 concentrations and the lower FeO and TiO_2 concentrations of the rocks. To elucidate the reasons for these differences, we calculated the mass-balance for the contents of minerals in the rock and their proportions relative to the residual melt (Table 12, calculation *2*). These data indicate that the amount of matrix glass in the rock is 34.9%, and those of olivine, pyroxene, plagioclase, and magnetite are 7.7, 10.3, 45.4, and 1.6%, respectively, which is consistent with the phase proportions of the rocks with regard for the contents of microlites in the groundmass. The comparison of the calculation results and cotectic proportions of the minerals during their crystallization from the parental melt (Table 12, calculation *1*) shows that the olivine and pyroxene contents are practically identical in both scenarios, the content of plagioclase in the rock and 10% higher and that of magnetite is 2% lower than those during the cotectic crystallization of the parental melt. We interpret these results as evidence that the contents of minerals in the basalt of the 1996 eruption do not correspond to the cotectic proportions. The rocks contain approximately 10% excess "xenogenic" plagioclase and are 2% deficient in magnetite. Correspondingly, the rocks show a pronounced minimum at Ti (magnetite deficit) and Sr/Ce ratios (excess plagioclase) higher than those in the melt inclusions, as can be seen in the normalized trace-element patterns (Fig. 6).

In order to explain the distinctive compositional features of the erupted magmas (i.e., rock compositions), we suggested the following model (Fig. 7). Upon the onset of the crystallization of the parental melt during its ascent, plagioclase, pyroxene, and olivine remained suspended in the magma and brought, together with the residual melt, to the surface. A minor amount (approximately 2%) of the most dense of the crystallizing phases (magnetite) was separated from the magma as a result of gravitational separation. To explain the excess content of plagioclase, we suggested that the magma entrained close to 10% plagioclase from earlier cumulates (for example, from the roof or apical part of the shallow-sitting chamber of Karymsky volcano) when ascending to the surface. Consequently, the integral composition of the erupted rocks became slightly richer in Al and poorer in both Ti and Fe than the parental melt.

Indirect evidence in support of the hypothesis that some plagioclase phenocrysts were borrowed from an older chamber of Karymsky volcano is provided by the fact that many melt inclusions in the plagioclase bear somewhat elevated concentrations of S, K, and particularly Li than those in inclusions in the olivine and pyroxene, with these concentrations approaching those in inclusions in the plagioclase from andesites of Karymsky volcano (Figs. 5, 6). Our data are insufficient to definitely decide as to which of the plagioclase phenocrysts crystallized *in situ* in the magma and which were borrowed from earlier cumulates, and to elucidate the nature of various plagioclase phenocrysts in the basalts erupted in 1996 is a challenging problem and a new possible avenue of the research.

Evaluated release of volatile components during the 1996 eruption. Our data on the concentrations of volatile components in the melts makes it possible to estimate the release of volatiles during the 1996 eruption at Karymskoe Lake. Since the composition of the volcanic rocks is close to that of the parental melts (see above), and the rocks contain no more that 10% excess plagioclase, the mass of the parental melt can be calculated from the volume of the erupted material (0.04 km^3). With regard for the density of basalt (~2.6 g/cm^3) and the porosity of the rocks (approximately 30%), the mass of the parental melt is estimated at approximately 7×10^7 t. Proceeding from the contents of volatile components of the parental melt (H_2O = 2.8 wt %, S = 0.20 wt %, and Cl = 0.084 wt %; Table 8), we evaluated the masses of the volatiles at 2.0×10^6 t for H_2O, 1.5×10^5 t for S, and 6.1×10^4 for Cl. The amount of matrix glass in the rocks is 45%. Hence, with regard for the concentrations of volatile components in the groundmass glass (Table 8), the amounts of volatiles retained in the residual melt should have been 3.7×10^5 t for H_2O, 9.9×10^3 t for S, and 4.6×10^4 t for Cl. The differences between the amounts of the volatiles in the quenched glasses and their original amounts in the magma should correspond to the amounts of these components released to the atmosphere and dissolved in Karymskoe Lake during the eruption. These amounts are as follows: $H_2O = 1.7 \times 10^6$ t, S = 1.4×10^5 t, and Cl = 1.5×10^4 t.

They suggest that 82% H_2O, 93% S, and 24% Cl (of their original amounts contained in the magma) escaped in the course of the eruption.

Our data allowed us to calculate the average emission rate of volatiles during the eruption at Karymskoe Lake, which lasted for 18 h. These estimates are as follows: $H_2O = 26$ t/s, S = 2.1 t/s, and Cl = 0.2 t/s and are a few orders of magnitude larger than the average emission of volatile components during the eruption of Karymsky volcano that continues until now. For example, according to [31], the sulfur emission from Karymsky volcano is close to 230 g/s, which is roughly 9000 times lower than the analogous value during the 1996 eruption. If the data in [31] are representative for the emission of volatiles at Karymsky volcano over the past 14 years, this means that since the 1996 eruption Karymsky volcano has emitted comparable or even lesser masses of volatile components than those released during the single brief eruption at Karymskoe Lake.

Genesis of the selectively Li-enriched inclusions in plagioclase. The anomalous Li enrichment of melt inclusions in plagioclase from andesites and basalts from the Karymsky center was first reported in [6]. A result obtained in the course of this research is that Li enrichment is selective and typical only of inclusions in plagioclase but not those in olivine or pyroxene. Also, inclusions in plagioclase, pyroxene, and olivine from basalts of the 1996 eruption bear practically identical concentrations of all major, trace (except Li), and volatile components. Among the examined inclusions, we failed to find any rich in Na and poor in Fe, which were earlier documented as inclusions in plagioclase from rocks from Karymsky center [2].

In order to explain Li enrichment in inclusions in plagioclase from the rocks, the following three distinct scenarios can be proposed: (1) crustal assimilation and the capture of Li-rich melts in plagioclase, (2) reequilibration of the melts with plagioclase at changes in the physicochemical parameters of the magma, and (3) reequilibration of the plagioclase with Li-rich melts/brines in the magmatic chamber [32].

Lithium is a mobile element in low-temperature processes, and several types of sedimentary rocks, especially, those rich in clay minerals and altered basalts, are enriched in Li [33]. The occurrence of resorbed quartz grains in the basalts erupted in 1996 and the presence of acid rock xenoliths entrained by the basalts during the eruption [4] testify that the magmas interacted with basement rocks. To explain the genesis of the Li-rich melts, it can be hypothesized that they were produced by the partial melting of altered host rocks. However, this requires that the Li-enriched melts should differ from the parental basaltic melts in concentrations of certain major and trace elements and should be entrapped in various minerals. In fact, melt inclusions in all of the examined minerals bear similar concentrations of major and trace elements except Li, which is hard to explain from the standpoint of the assimilation of crustal material.

A possible alternative explanation is the diffusion-controlled reequilibration of inclusions in plagioclase, which originally had the same composition as inclusions in olivine and pyroxene, with the host mineral at changes in the temperature of the ambient melt. However, available experimental data indicate that the Li partition coefficient of plagioclase and melt (D_{Li}) is practically independent of the concentration of the anorthite component in the plagioclase, is little sensitive to temperature, and is 0.14–0.27 at temperatures of 1150–1300°C [34]. Our data indicate that the melts crystallized within a narrow temperature range of 1030–1060°C (Table 8). Temperature variations within 30°C obviously could not create variations in D_{Li} by a factor of four as is required for explaining the enrichment of inclusions in plagioclase compared to those in olivine and pyroxene.

The selective Li enrichment of plagioclase, amphibole, and melt inclusions in these minerals was documented in detail in andesite from St. Helens volcano [32, 35, 36]. It was hypothesized that Li and other alkaline elements are mobilized into the fluid phase during magma degassing at intermediate levels of the magmatic chamber under a pressure of about 2 kbar. This fluid migrated to the upper levels of the chamber and gave rise to a dense Li-rich salt melt (brine) and low-density H_2O-rich fluid at retrograde boiling under a pressure of approximately 1 kbar. The low-density fluid escaped from the magmatic chamber, whereas the less mobile salt melts were accumulated at the roof of the magmatic chamber and were reequilibrated with the ambient melt and minerals. As was demonstrated in [37], Li diffusion in plagioclase is a very fast process ($\log D_o^{Li} = -3.8$ m/s^2), and this results in more than 90% reequilibration of plagioclase crystals 1–2 mm long with the melt during a time span of a few days [32]. Other alkaline elements, which were also mobilized by the fluid phase, could not as rapidly diffuse in Ca-rich plagioclase (for example, $\log D_o^{Rb} = -5.8$ m/s^2 [37]). During the same time span, the degree of reequilibration of plagioclase with the surrounding melt in these elements would not exceeds 1%.

With reference to the melt inclusions, the model of diffusion-controlled reequilibration with Li-rich brines/melts is able to realistically account for the selective Li enrichment of inclusions in plagioclase. The reason for this selective enrichment could be the aforementioned extremely fast diffusion of Li in plagioclase, whereas Li diffusion in olivine and pyroxene [38, 39] is a few orders of magnitude slower process. Because of this, inclusions in pyroxene and olivine likely had not enough time to reequilibrate their Li concentration with the ambient melt.

A more important problem to be solved is the fact that the matrix melt of the rocks has lower Li concentrations, which cannot explain Li enrichment in the inclusions in plagioclase. Hence, Li-rich melts/brines should have interacted with preexisting crystals during an earlier fractionation process, after which they were replaced (for an uncertain reason) by a matrix melt of usual composition. Moreover, it is unclear so far as to where and when the crystals could have been reequilibrated. All available petrological data reported above testify that crystallization was a brief process during magma ascent to the surface. Thereby it is unlikely that the magma could reside somewhere and then interact with Li-rich melts/brines, which vanished thereafter without leaving any traces.

These problems could be settled by assuming that not all plagioclase crystals of the rock were reequilibrated with Li-rich melts/brines. As was discussed above, the basalts erupted in 1996 contain approximately 10% excess plagioclase, which was likely captured by the magma from earlier cumulates. It can be suggested that these exactly plagioclases were reequilibarted, when occurring in the chamber, with Li-rich melts/brines before the 1996 eruption. We cannot rule out that the inclusions analyzed for trace elements were obtained from this exactly plagioclase population.

This hypothesis can be tested by the statistical analysis of Li concentrations in plagioclase crystals contained in the rocks erupted in 1996 with the aim of detecting possible zonal Li distribution in the plagioclase crystals and evaluating the proportions of the Li-rich and Li-poor crystals. If the model suggested above is valid, then close to 75% of plagioclase crystals in the basalts erupted in 1996 should have Li concentrations lower than those in equilibrium with the matrix melt (<2.5 ppm). The Li concentrations of the xenocrysts should be higher than this value.

CONCLUSIONS

We have examined the composition of more than 200 glassy melt inclusions in phenocrysts of olivine (Fo_{82-72}), plagioclase (An_{92-73}), and clinopyroxene ($Mg\#$ 83–70) from basalts erupted in 1996 at Karymskoe Lake. These data allowed us to estimate the changes in the physicochemical parameters of the magma before its eruption and led us to draw certain conclusions providing insight into the near-surface evolution of arc magmas and the nature of explosive basaltic volcanism. The principal conclusions of our studies are as follows:

The parental melt of the 1996 eruption corresponded to low-Mg high-Al basalt (SiO_2 = 50.2 wt %, MgO = 5.6 wt %, Al_2O_3 = 17 wt %) of mildly potassic type (K_2O = 0.56 wt %) and contained much volatile components (H_2O = 2.8 wt %, S = 0.20 wt %, Cl = 0.084 wt %).

The compositions of melt inclusions in the three minerals are similar and suggest that the olivine, plagioclase, and pyroxene crystallized simultaneously, starting at pressures of approximately 1.5 kbar, under varying pressure, at temperature varying within a narrow range of 1030–1060°C; the crystallization process terminated at a pressure of approximately 100 bar. Mass crystallization was triggered by H_2O degassing from the melt under pressures of less than 1 kbar. The degree of crystallization of the magma at the moment of its eruption was 55%. The rocks contain phenocryst minerals in proportions deviating from the cotectic ones due to the entrainment of approximately 10% "xenogenic" plagioclase phenocrysts and the loss of nearly 2% magnetite when the magma ascended to the surface.

Magma degassing in an open system resulted in the escape of 82% of its initial H_2O amount in the magma, 93% S, and 24% Cl. The emission of the volatiles to the atmosphere during the eruption, which lasted 18 h, amounted to 1.7×10^6 t for H_2O, 1.4×10^5 t for S, and 1.5×10^4 t for Cl. The escape of volatiles to the atmosphere during the 1996 eruption was approximately 9000 times more intense than this process during the ongoing eruption of Karymsky volcano.

The concentrations of most incompatible trace elements in the melt inclusions are close to those in the rocks, and the variations in these concentrations are close to those expected to occur during the fractionation of olivine, plagioclase, pyroxene, and magnetite. Selective Li enrichment was detected in melt inclusions contained in plagioclase; the Li concentrations in these inclusions are four times as high as in melt inclusions in the pyroxene and olivine. The Li-enriched plagioclase and melt inclusions in it are thought to be entraped from cumulus layers in the feeding system beneath Karymsky volcano, in which plagioclase crystals interacted with a Li-rich melt/brine and were subsequently entrained by magma during the 1996 eruption.

ACKNOWLEDGMENTS

The authors thank A.B. Belousov and M.G. Belousova for providing rock samples for this study. Much help in the analytical work was provided by S.G. Simakin and E.V. Potapov. A.A. Ariskin was one of the supervisors of I.A. Belousov's graduation research at the Moscow State University, which was defended at the University in 2005 and whose materials provided the basis for this study. The authors thank P.Yu. Plechov and A.A. Ariskin for comments on and constructive criticism of an early version of the manuscript.

This study was financially supported by the KALMAR Russian–German project, which is financed by Germany, the Russian Foundation for Basic Research (project nos. 07-05-00807, 07-05-00497, 09-05-01234, and 10-05-00209), Russian Federal Agency for Science and Innovations (GK

02.515.12.5016), and the Council on Research Grants at the President of the Russian Federation for the support of leading research schools (Grants NSH-150.2008.5 and NSH-3919.2010.5).

REFERENCES

1. E. N. Grib, "Petrology of Products of January 2–3, 1996 Eruption in the Akademii Nauk Caldera," Vulkanol. Seismol., No. 5, 71–96 (1997).
2. M. L. Tolstykh, V. B. Naumov, A. Yu. Ozerov, and N. N. Kononkova, "Composition of Magmas of the 1996 Eruption at the Karymskii Volcanic Center, Kamchatka: Evidence from Melt Inclusions," Geochem. Int. **39**, 447–458 (2001).
3. P. E. Izbekov, J. C. Eichelberger, L. C. Patino, et al., "Calcic Cores of Plagioclase Phenocrysts in Andesite from Karymsky Volcano: Evidence for Rapid Introduction by Basaltic Replenishment," Geology **30**, 799–802 (2002).
4. P. E. Izbekov, J. C. Eichelberger, and B. V. Ivanov, "The 1996 Eruption of Karymsky Volcano, Kamchatka: Historical Record of Basaltic Replenishment of An Andesite Reservoir," J. Petrol. **45**, 2325–2345 (2004).
5. P. Izbekov, J. Gardner, and J. Eichelberger, "Comagmatic Granophyre and Dacite from Karymsky Volcanic Center, Kamchatka: Experimental Constraints for Magma Storage Conditions," J. Volcanol. Geotherm. Res. **131**, 1–18 (2004).
6. V. B. Naumov, M. L. Tolstykh, E. N. Grib, et al., "Chemical Composition, Volatile Components, and Trace Elements in Melts of the Karymskii Volcanic Center, Kamchatka, and Golovnina Volcano, Kunashir Island: Evidence from Inclusions in Minerals," Petrology **16**, 1–18 (2008).
7. I. N. Bindeman, V. V. Ponomareva, J. C. Bailey, and J. W. Valley, "Volcanic Arc of Kamchatka: A Province with High-^{18}O Magma Sources and Large-Scale $^{18}O/^{16}O$ Depletion of the Upper Crust," Geochim. Cosmochim. Acta **68**, 841–865 (2004).
8. A. Gorbatov, V. Kostoglodov, G. Suarez, and E. Gordeev, "Seismicity and Structure of the Kamchatka Subduction Zone," J. Geophys. Res. **102**, 17833–17898 (1997).
9. B. V. Ivanov, *1962–1965 Eruption at Karymsky Volcano and Volcanoes of the Karymsky Group* (Nauka, Moscow, 1970) [in Russian].
10. O. A. Braitseva and I. V. Melekestsev, "Karymsky Volcano: Evolution, Activity Dynamics, and Long-Term Prediction," Vulkanol. Seismol., No. 2, 14–31 (1989).
11. I. Bindeman, V. L. Leonov, P. E. Izbekov, et al., Large-Volume Silicic Volcanism in Kamchatka: Ar–Ar, U–Pb ages and Geochemical Characteristics of Major pre-Holocene Caldera-Forming Eruptions, J. Volcanol. Geotherm. Res. **189**, 57–80 (2010).
12. Ya. D. Murav'ev, S. A. Fedotov, V. A. Budnikov, et al., "Volcanic Activity in the Karymsky Center in 1996: Summit Eruption of Karymsky Volcano and Phreatmagmatic Eruption in the Akademii Nauk Caldera," Vulkanol. Seismol., No. 5, 38–70 (1997).
13. A. Belousov and M. Belousova, "Eruptive Process, Effects and Deposits of the 1996 and the Ancient Basaltic Phreatomagmatic Eruptions in Karymskoye Lake, Kamchatka, Russia," Spec. Publ. Int. Ass. Sediment **30**, 35–60 (2001).
14. E. J. Jarosewich, J. A. Nelen, and J. A. Norberg, "Reference Samples for Electron Microprobe Analysis," Geostand. Newslett. **4**, 43–47 (1980).
15. A. V. Sobolev, "Melt Inclusions in Minerals as a Source of Principle Petrological Information," Petrology **4**, 209–220 (1996).
16. M. V. Portnyagin, K. Hoernle, P. Y. Plechov, et al., "Constraints on Mantle Melting and Composition and Nature of Slab Components in Volcanic Arcs from Volatiles (H_2O, S, Cl, F) and Trace Elements in Melt Inclusions from the Kamchatka Arc," Earth Planet. Sci. Lett. **255**, 53–69 (2007).
17. A. B. E. Rocholl, K. Simon, K. P. Jochum, et al., "Chemical Characterization of NIST Silicate Glass Certified Reference Material SRM 610 by ICP-MS, TIMS, LIMS, SSMS, INAA, AAS and PIXE," Geostand. **21**, 101–114 (1997).
18. K. P. Jochum, B. Stoll, M. Willbold, et al., "MPI-DING Reference Glasses for in Situ Microanalysis: New Reference Values for Element Concentrations and Isotope Ratios," Geochem. Geophys. Geosyst. **7** (2006).
19. L. Danyushevsky, A. W. McNeill, and A. V. Sobolev, "Experimental and Petrological Studies of Melt Inclusions in Phenocrysts from Mantle-Derived Magmas: An Overview of Techniques, Advantages and Complications," Chem. Geol. **183**, 5–24 (2002).
20. J. B. Gill, *Orogenic Andesites and Plate Tectonics* (Springer, Berlin-Heidelberg, 1981).
21. C. E. Ford, D. G. Russel, J. A. Graven, and M. R. Fisk, "Olivine-Liquid Equilibria: Temperature, Pressure and Composition Dependence of the Crystal/Liquid Cation Partition Coefficients for Mg, Fe^{2+}, Ca and Mn," J. Petrol. **24**, 256–265 (1983).
22. R. R. Almeev, F. Holtz, J. Koepke, et al., "The Effect of H_2O on Olivine Crystallization in MORB: Experimental Calibration at 200 MPa," Am. Mineral. **92**, 670–674 (2007).
23. S.-S. Sun and W. F. McDonough, "Chemical and Isotopic Systematics of Oceanic Basalts: Implications for Mantle Composition and Processes," in *Magmatism in the Ocean Basins*, Ed. by A. D. Saunders and M. J. Norry, Geol. Soc. Sp. Publ. London **42**, 313–345 (1989).
24. S. Newman and J. B. Lowenstern, "VOLATILECALC: a Silicate Melt–H_2O–CO_2 Solution Model Written in Visual Basic for Excel," Comp. Geosci. **28**, 597–604 (2002).
25. A. V. Sobolev, V. S. Kamenetskii, N. Metrik, et al., "Regime of Volatiles and Conditions of Crystallization of Hawaiite Lavas of Etna Volcano, Sicily," Geokhimiya, No. 9, 1277–1290 (1990).
26. T. W. Sisson and T. L. Grove, "Temperatures and H_2O Contents of Low-MgO High-Alumina Basalts," Contrib. Mineral. Petrol. **113**, 167–184 (1993).
27. N. L. Mironov, M. V. Portnyagin, P. Yu. Plechov, and S. A. Khubunaya, "Final Stages of Magma Evolution in Klyuchevskoy Volcano, Kamchatka: Evidence from Melt Inclusions in Minerals of High-Alumina Basalts," Petrology **9**, 46–62 (2001).

28. J. Blundy, K. Cashman, and M. Humphrys, "Magma Heating by Decompression-Driven Crystallization Beneath Andesite Volcanoes," Nature **443**, 76–80 (2006).

29. J. A. Wade, T. Plank, W. G. Melson, et al., "The Volatile Content of Magmas from Arenal Volcano, Costa Rica," J. Volcanol. Geotherm. Res. **157**, 94–120 (2006).

30. P. J. Wallace, "Volatiles in Subduction Zone Magmas: Concentrations and Fluxes Based on Melt Inclusion and Volcanic Gas Data," J. Volcanol. Geotherm. Res **140**, 217–240 (2005).

31. T. P. Fischer, K. Roggensack, and P. R. Kyle, "Open and Almost Shut Case for Explosive Eruptions: Vent Processes Determined by SO_2 Emission Rates at Karymsky Volcano, Kamchatka," Geology **30**, 1059–1062 (2002).

32. A. J. R. Kent, J. Blundy, K. V. Cashman, et al., "Vapor Transfer prior to the October 2004 Eruption of Mount St. Helens, Washington," **35**, 231–234, (2007).

33. C. Bouman, T. Elliott, and P. Z. Vroon, "Lithium Inputs to Subduction Zones," Chem. Geol. **212**, 59–79 (2004).

34. I. N. Bindeman, A. M. Davis, and M. J. Drake, "Ion Microprobe Study of Plagioclase–Basalt Partition Experiments at Natural Concentration Levels of Trace Elements," Geochim. Cosmochim. Acta **62**, 1175–1193 (1998).

35. K. Berlo, J. Blundy, S. Turner, et al., "Geochemical Precursors to Volcanic Activity at Mount St. Helens, USA," Science. **306**, 1167–1169 (2004).

36. M. C. Rowe, A. J. R. Kent, and C. R. Thornber, "Using Amphibole Phenocrysts to Track Vapor Transfer during Magma Crystallization and Transport: An Example from Mount St. Helens, Washington," J. Volcanol. Geotherm. Res. **178**, 593–607 (2008).

37. B. J. Giletti and T. M. Shanahan, "Alkali Diffusion in Plagioclase Feldspar," Chem. Geol. **139**, 3–20 (1997).

38. R. Dohmen, S. A. Kasemann, L. Coogan, and S. Chakraborty, "Diffusion of Li in Olivine. Part I: Experimental Observations and a Multi Species Diffusion Model," Geochim. Cosmochim. Acta **74**, 274–292 (2010)

39. L. A. Coogan, S. A. Kasemann, and S. Chakraborty, "Rates of Hydrothermal Cooling of New Oceanic Upper Crust Derived from Lithium-Geospeedometry," Earth Planet. Sci. Lett. **240**, 415–424 (2005).